Thymus-Derived Regulatory T Cells Are Positively Selected on Natural Self-Antigen through Cognate Interactions of High Functional Avidity

Thymus-derived regulatory T cells are positively selected on natural self-antigen through TCR interactions of high functional avidity

Elisa Kieback[1,2,*], Ellen Hilgenberg[3,*], Ulrik Stervbo[3], Vicky Lampropoulou[3], Ping Shen[3], Mario Bunse[2], Yarua Jaimes[3], Pierre Boudinot[4], Andreas Radbruch[3], Uwe Klemm[5], Anja A. Kühl[6], Roland Liblau[7], Nadine Hoevelmeyer[8], Stephen M. Anderton[9], Wolfgang Uckert[1,2], Simon Fillatreau[3,10,11,12]

[1]Humboldt University of Berlin, Institute of Biology, D-10115 Berlin, Germany

[2]Max-Delbrueck-Center for Molecular Medicine in the Helmholtz Association, D-13125 Berlin, Germany

[3]Deutsches Rheuma-Forschungszentrum, a Leibniz Institute, D-10117 Berlin, Germany

[4]INRA, Unité de Virologie et Immunologie Moléculaire, F-78352 Jouy en Josas, France

[5]Max Planck Institute of Infection Biology, D-10117 Berlin, Germany

[6]Institute of Pathology/RCIS, Charité, Campus Benjamin Franklin, D-12203 Berlin, Germany

[7]CPTP, INSERM UMR 1043 / CNRS UMR 5282, Université Toulouse III, F-31024 Toulouse, France

[8]Institute for Molecular Medicine, Johannes Gutenberg University of Mainz, D-55131 Mainz, Germany

[9]MRC Centre for Inflammation Research, University of Edinburgh, The Queens Medical Research Institute, Edinburgh, EH16 4TJ, Great Britain

[10]Institut Necker-Enfants Malades (INEM), INSERM U1151-CNRS UMR 8253, Paris, France

[11]Université Paris Descartes, Sorbonne Paris Cité, Faculté de Médecine, Paris, France

[12]Assistance Publique - Hôpitaux de Paris (AP-HP), Hôpital Necker Enfants Malades, Paris, France

Corresponding author:

Simon Fillatreau

Institut Necker Enfants-Malades (INEM)

Equipe 16 - Immunity in Health and Disease

14 Rue Maria Helena Vieira da Silva

75993 Paris Cedex 14

France

Tel: +33 (0) 1 72 60 64 85

Fax: +33 (0) 1 72 60 64 01

E-mail: simon.fillatreau@inserm.fr

Footnotes:

* These two authors contributed equally to the work

SUMMARY

Regulatory T cells (Tregs) expressing Foxp3 are essential for immune homeostasis. They arise in the thymus as a separate lineage from conventional $CD4^+Foxp3^-$ T cells (Tconvs). Here, we show that the thymic development of Tregs depends strongly on the expression of their endogenous cognate self-antigen. The formation of these cells was significantly impaired in mice lacking this self-antigen, while Tconv development was not negatively affected. Thus, some thymus-derived Tregs are selected by self-antigens in a specific manner, while autoreactive Tconvs are produced through degenerate recognition of distinct antigens. These distinct modes of development were associated with the expression of T cell receptor of higher functional avidity for self-antigen by Tregs than Tconvs, a difference subsequently essential for the control of autoimmunity in the periphery. Overall, our study documents how self-antigens define the repertoire of thymus-derived Tregs to subsequently endow this cell type with the capacity to undermine autoimmune attacks.

INTRODUCTION

$CD4^+$ T regulatory cells (Tregs) expressing Foxp3 play an essential role in immune homeostasis. Humans bearing null-mutations in the *FOXP3* gene display a deficit in Tregs, and develop the fatal immunodysregulation polyendocrinopathy enteropathy X-linked syndrome (IPEX) early in childhood (Bennett et al., 2001). Similarly, deficiency in the *Foxp3* gene in mice results in a lack of Tregs, and lethal immunopathology (Fontenot et al., 2003).

The inhibition of immunity by Tregs necessitates their activation via the T cell receptor (TCR) (Levine et al., 2014). The antigens stimulating Treg activation at steady state must be self-antigens because Tregs restrain immune-mediated pathogenesis also in germ-free mice (Chinen et al., 2010).

The antigen recognition properties of Tregs are largely defined during their development in the thymus (Hsieh et al., 2006; Pacholczyk et al., 2006). Experiments performed with Nur77-eGFP reporter mice indicated that Tregs received stronger TCR signals than $CD4^+Foxp3^-$ conventional T cells (Tconvs) during their thymic development (Moran et al., 2011). Accordingly, a study using “TCR-cognate antigen” double-transgenic mice showed that a TCR with high affinity for the selecting antigen drove Treg development, while other TCR of low affinity did not (Jordan et al., 2001). A role for strong TCR signalling during early Treg specification might be to promote the expression of TNF receptor super-family members GITR, OX40, and TNFR2, which facilitate Treg formation (Mahmud et al., 2014), and to stimulate the

epigenetic changes of the *Foxp3*, *Ctla4*, *Il2ra*, and *Itgal* loci associated with Tregs (Morikawa and Sakaguchi, 2014).

The nature of the cognate antigens governing Treg selection in the thymus remains controversial. None of the studies mentioned above addressed this issue as they were either performed using artificial transgenic antigens (Jordan et al., 2001) or only provided indication on the intensity of the TCR signalling associated with Treg formation in response to non-defined epitopes (Moran et al., 2011). Although self-antigens are regularly evoked as mediators of this process, no self-antigen that selects Tregs has been identified. Moreover, this concept has been repeatedly questioned, and some investigators claimed that microbiota was the primary source of antigens mediating Treg selection (van Santen et al., 2004, Pennington et al., 2006, Pacholczyk et al., 2007).

Here, we sought to investigate the identity of the antigens implicated in Treg thymic selection. We focused on Tregs specific for myelin oligodendrocyte glycoprotein (MOG), a minor component of the myelin sheath that is an important target in autoimmune diseases of the central nervous system (CNS). Upon activation, $CD4^+$ T cells reacting against MOG can provoke an inflammatory demyelinating disease of the CNS in mice, called experimental autoimmune encephalomyelitis (EAE), which is the primary pre-clinical model for multiple sclerosis (Fillatreau et al., 2002). In this disease, MOG-reactive Tregs provide an essential mechanism of protection from immune-mediated pathogenesis (McGeachy et al., 2005). We demonstrate

that endogenous MOG expression contributes significantly to the thymic development of MOG-reactive Tregs. We also show that these Tregs express TCR of higher functional avidity for MOG than Tconvs, and reveal the importance of this difference for the regulation of autoimmunity.

RESULTS

A TCRβ transgenic mouse to study MOG-reactive Tconvs and Tregs

Autoreactive Tconvs differ in their capacity to cause autoimmune disease. Those expressing public TCR clonotypes are prominent drivers of pathogenesis (van den Elzen et al., 2004). In order to analyse such cells, we generated a transgenic mouse (named Kaa mouse) expressing the public TCRβ clonotype of the MOG-reactive $CD4^+$ T cell response during EAE in C57BL/6 mice (Fazilleau et al., 2006). This public TCRβ chain contains a Vβ8.2 segment (Figure S1A), which is expressed in both Tconvs and Tregs in the CNS of C57BL/6 mice with EAE (Figure S1B).

Naïve Kaa mice contained an increased frequency of MOG-reactive Tconvs, estimated at around 1.8% in spleen using CD40L expression as indicator of TCR stimulation (Figure S1C) (Frentsch et al., 2005). Kaa Tconvs were encephalitogenic because cells isolated from lymph nodes (LN) of Kaa mice immunized with MOG(35-55) expressed IFN-γ as well as TNF-α upon *ex vivo* re-stimulation, and induced EAE in recipient mice upon adoptive transfer (Figure 1A). Tconvs from naïve Kaa mice stimulated under the same condition also induced EAE in recipient mice, while non-transgenic Tconvs had no effect (Figure 1B).

Despite harbouring encephalitogenic Tconvs, Kaa mice developed a milder EAE than wild-type mice upon immunization with MOG(35-55) (Figure 1C). We hypothesized that the Kaa mouse contained elevated numbers of MOG-reactive Tregs. Using MOG-I-A(b) tetramers we found that 7.2 % of

Tregs were MOG-reactive in the LN of Kaa.Foxp3.IRES.eGFP mice (Figure 1D). These Tregs were functional since the proliferation of Kaa T cells stimulated with MOG(35-55) was increased after Treg depletion (Figure 1E), and adoptive transfer of Kaa Tregs improved the course of EAE in recipient C57BL/6 mice, while non-transgenic Tregs had no effect (Figure 1F). This protection was associated with an accumulation and proliferation of adoptively transferred Kaa Tregs in the draining LN of recipient mice immunized with MOG(35-55), which was not observed in control groups (Figure 1G and S1D). Moreover, interfering with Treg function in Kaa mice exacerbated EAE (Figure 1H). Collectively, these data demonstrate that Kaa mice contain protective MOG-reactive Tregs that efficiently counteract encephalitogenic MOG-reactive Tconvs.

Antigen recognition properties of Tconvs and Tregs in the Kaa mouse

Tregs and Tconvs express distinct TCR repertoires in wild-type mice (Hsieh et al., 2006; Pacholczyk et al., 2006), suggesting that they differ in their antigen recognition properties. We sought to address whether this was the case for cells specific for a disease-relevant autoantigen.

To characterize the TCRα chains expressed by disease-relevant MOG-reactive Tregs and Tconvs, we induced EAE in Kaa mice on a Foxp3.IRES.eGFP.TCR$\beta^{+/-}$TCR$\alpha^{+/-}$ background, and isolated $CD4^+GFP^+$ cells (Tregs) as well as $CD4^+GFP^-$ cells (Tconvs) from their CNS at the peak of disease. TCRα sequences were amplified from these cells using a 5' RACE PCR to allow unbiased repertoire analysis. Three independent experiments

were performed, yielding a total of 3592 and 3928 TCRα sequences, which corresponded to 1011 and 1086 unique TCRα sequences for Tregs and Tconvs, respectively. We focused our analyses on sequences found in each of the three samplings for Tregs or Tconvs, assuming that these would derive from disease-relevant MOG-reactive cells. This yielded 21 and 22 TCRα for Tconvs and Tregs, respectively (Figure S2A), corresponding to 40 distinct TCRα (three sequences were present in both subsets). Importantly, the frequency of these TCRα among the total number of sequences analysed for each experiment confirmed their biased representation in the Treg or Tconv compartments (Figure 2A).

We could re-express 30 of these 40 TCRα (Figure S2B and Table S1) together with the Kaa TCRβ in a TCR-deficient cell line that produced IL-2 proportionally to the strength of stimulation of the ectopic TCR (Letourneur and Malissen, 1989). The majority of the TCR tested (28/30) were MOG-reactive (Figure S2B). The TCR from Tregs (n=17) conferred the cell line a markedly stronger reactivity towards MOG than did Tconv-derived TCR (n=11) (Figure 2B). The bi-modal distribution of this response shows that TCR of Tregs and Tconvs belong to two distinct classes differing by their functional avidity for MOG.

To assess if this difference in functional avidity was associated with qualitative differences in the recognition of the antigen, we evaluated whether distinct residues within MOG(35-55) were important for stimulating Treg versus Tconv TCR. First, we activated a sample of the cell lines expressing

TCR from Tregs (n=7) or Tconvs (n=6) with modified MOG(35-55) peptides containing alanine substitutions at each of the 21 amino acid positions, and quantified their IL-2 production relative to the response elicited by the original MOG(35-55) peptide (Figure S2C). Based on the obtained results, we then focused on six altered peptides that affected the cell lines expressing TCR from Tregs and Tconvs in a distinct manner (Figure S2C), and re-tested them on the 28 cell lines available (Figure 2C). Five of these peptides elicited distinct IL-2 responses depending on the origin of the TCR expressed by the cell lines. In particular, the 49(H→A) peptide increased the amount of IL-2 produced by cell lines expressing Tconv TCR by about 10-fold while having little effect on the response of cells bearing Treg TCR. From these results, we conclude that the TCR from Tregs and Tconvs characterized in this study differently recognize the MOG antigen with conserved properties within each class.

A limitation of the clonal analyses described above is that they are only feasible for a limited number of TCR. In an attempt to generalize these findings, we tested the prediction that the 49(H→A) peptide should be more encephalitogenic than the original self-antigen because it was a stronger Tconv stimulant. Indeed, the variant 49(H→A) induced a more severe EAE than the original MOG(35-55) peptide (Figure 2D), correlating with the induction of stronger encephalitogenic $CD4^+$ T cell responses (Figure 2E). These results corroborate the notion that Tconvs and Tregs carry TCR with different antigen recognition properties.

Instructive role of the TCR for the development of MOG-reactive Tregs

We evaluated the capacities of TCR cloned from MOG-reactive Tregs and Tconvs to drive Treg development *in vivo* generating TCR retrogenic mice using six TCR from Tregs and six TCR from Tconvs.

Donor-derived $CD4^+$ T cells were detected in the blood of retrogenic mice starting two weeks after reconstitution, and followed distinct patterns of repopulation depending on the origin of the TCR. Donor-derived $CD4^+$ T cell numbers were lower (Figure 3A), while Treg frequencies were higher (Figure 3B) in mice prepared with TCR from Tregs compared to those produced with TCR from Tconvs. Similar differences were observed in thymus and spleen (Figure 3C), as well as LN (Figure S3A), both in frequency and absolute number of Tregs. Thus, TCR from MOG-reactive Tregs generate Tregs more efficiently than TCR from Tconvs. In line with previous studies, however, none of the TCR induced the formation of only Tregs (Bautista et al., 2009; Leung et al., 2009).

We then measured expression of Helios, a transcription factor of the Ikaros family described as a marker of thymus-derived Tregs (Thornton et al., 2010). Nearly all donor-derived Tregs expressed Helios in mice made with Treg TCR, while fewer Tregs expressed Helios in mice generated with TCR from Tconvs (Figure 3D). As expected, Tconvs did not express Helios (Figure S3B). Further cytometric analyses indicated that donor-derived Tregs were mostly $CD25^+CD62L^+GITR^{high}$ irrespective of the origin of their TCR, while Tconvs displayed different phenotypes (Figure S3C).

Taken together, our results show that TCR of high functional avidity for MOG have a superior capacity to generate Helios-expressing Tregs.

Endogenously expressed MOG controls the development of MOG-reactive Tregs

The role of self-antigens in Treg development remains controversial. Here, we examined whether MOG was required for the formation of MOG-reactive Tregs using *Mog*-deficient mice (Hovelmeyer et al., 2005).

We selected four Treg-derived TCR to prepare retrogenic mice using wild-type and *Mog*-deficient mice as recipients. Absolute numbers and frequencies of Tregs among donor-derived $CD4^+$ T cells were reduced in the thymus of *Mog*-deficient mice compared to controls (Figure 4A). Similar differences were observed in spleens and LN, although they were less striking for some TCR (Figure 4B and S4A). Fewer donor-derived Tregs expressed Helios in *Mog*-deficient mice, compared to controls, illustrating the contribution of MOG to the normal development of MOG-reactive Tregs (Figure 4C and S4B). Expression of CD25, CD62L, or GITR was in contrast not influenced by MOG (Figure S4C-E).

To address how endogenous MOG expression influenced the development of MOG-reactive Tregs in a polyclonal setting, we reconstituted wild-type and *Mog*-deficient mice with bone marrow cells from Kaa.Foxp3.IRES.eGFP mice, and used MOG-I-A(b) tetramer to quantify

MOG-reactive Tregs and Tconvs (Figure 4D). The frequency of MOG-I-A(b)-binding cells among $CD4^+GFP^+$ Tregs, and the absolute number of MOG-I-A(b)-binding $CD4^+GFP^+$ Tregs were markedly reduced (absolute number reduced by 42%) in the thymus of *Mog*-deficient mice compared to controls (Figure 4D). These results show that the absence of a single self-antigen, here MOG, is sufficient to reduce the formation of MOG-reactive Tregs.

In contrast, MOG-reactive Tconvs were efficiently selected in the absence of MOG. They were present in similar numbers in wild-type and *Mog*-deficient retrogenic mice (Figure S4F), and were more abundant in the thymus of the chimera mice bearing a polyclonal repertoire that lacked MOG expression compared to controls (Figure 4E). Thus, distinct cognate antigens control the formation of MOG-reactive Tregs and Tconvs in the thymus.

TCR functional avidity controls the activity of Tregs and Tconvs during autoimmune disease

We next addressed whether the function of Tregs and Tconvs in the periphery was influenced by the functional avidity of their TCR for the disease-relevant self-antigen.

First, we ectopically expressed two MOG-reactive TCR from Tregs and two MOG-reactive TCR from Tconvs in polyclonal Tconvs through TCR gene transfer (Figure 5A). Although the four T cell populations displayed similar IFN-γ production upon stimulation with PMA/Ionomycin (Figure S5A), those expressing a TCR from Tregs produced more IFN-γ upon stimulation with

MOG(35-55) (Figure 5B). Upon adoptive transfer, these four Tconv populations expanded comparably in recipient mice (Figure 5C). However, Tconvs expressing a TCR from Tregs caused a more severe EAE in recipient mice with an earlier disease onset (Figure 5D) and a higher cumulative disease burden (Figure S5B). Thus, the functional avidity of their TCR for MOG determines the encephalitogenic potential of Tconvs.

We next ectopically expressed the same four TCR in polyclonal Tregs (Figure 5E). Upon activation with MOG(35-55), such engineered Tregs suppressed responder T cell proliferation in a dose-dependent manner *in vitro* (Figure S5C). Upon adoptive transfer, Tregs expressing a TCR of high avidity for MOG afforded better protection from EAE than Tregs carrying a low avidity TCR (Figure 5F and S5D), correlating with a stronger reduction of the autoreactive T cell response in recipient mice (Figure 5G). We conclude that the functional avidity of their TCR for MOG determines the protective function of Tregs in EAE.

Therapeutic function of engineered Tregs

We next characterized how polyclonal Tregs expressing a TCR of high functional avidity for MOG protected recipient mice from EAE in a prophylactic setting, and determined whether these Tregs were also beneficial when adoptively transferred after, or long before, EAE induction.

In a prophylactic setting the protection afforded by engineered Tregs was associated with their accumulation (Figure S6A), and a reduced

encephalitogenic T cell response (Figure 6A) in the draining LN of recipient mice. The transferred Tregs also migrated to the CNS of recipient mice (Figure S6B), correlating with a decreased inflammatory immune cell infiltrate (Figure 6B and S6C). Thus, the engineered Tregs suppressed the pathogenic reaction in both secondary lymphoid organs and the target tissue. Transduced Tregs still reduced disease severity when administered in recipient mice at EAE onset (Figure 6C). They also persisted long-term after transfer in naïve recipient mice (Figure S6D), and when these mice were immunized six weeks after Treg transfer, the latter cells reduced the activation of the pathogenic T cell response (Figure S6E), the progression of EAE course (Figure 6D), and disease-associated mortality (Figure S6F). We conclude that polyclonal Tregs engineered to express a TCR of high functional avidity for a disease-relevant antigen might provide a cellular therapy to treat diseases caused by unwanted T cell responses.

CTLA-4 expression is essential for the suppressive function of Tregs engineered with TCR of high functional avidity

We next asked whether polyclonal Tregs activated *ex vivo* and genetically engineered to express a TCR of high functional avidity for MOG remained reliant on mechanisms commonly used by Tregs to suppress immunity.

CTLA-4 is pivotal for Treg-mediated suppression (Wing et al., 2008), even though one study found that it was dispensable for the limitation of CNS autoimmunity (Verhagen et al., 2009). To produce MOG-reactive Tregs having reduced levels of CTLA-4 we developed a retroviral vector containing

the MOG-reactive TCR cassette and two miRNA to knockdown CTLA-4 (Figure 7A). The knockdown of CTLA-4 (Figure 7B) abolished the protection afforded by MOG-reactive Tregs (Figure 7C). These Tregs retained low CTLA-4 levels in recipient mice (Figure 7D), and expanded less than control MOG-reactive Tregs (Figure 7E). Thus, CTLA-4 is essential for the therapeutic effect of engineered Tregs against EAE. In contrast, knockdown of CD49d or GITR (Figure 7B) did not impair the protective effect of MOG-reactive Tregs (Figure 7C). It is remarkable that CD49d seems dispensable for the protective function of adoptively transferred Tregs, because this integrin is essential for the infiltration of pathogenic T cells into the CNS (Yednock et al., 1992).

DISCUSSION

The antigens selecting thymus-derived Tregs remain poorly defined. Here, we report the identification of a natural self-antigen controlling the generation of thymus-derived Tregs. Moreover, we document how differences in the properties of the TCR instructing Tregs development, compared to those producing Tconvs, contribute to limit the risk of autoimmunity.

It is striking that the absence of a single antigen, MOG, resulted in a marked loss of MOG-reactive Tregs in the thymus because it is generally admitted that TCR recognition of antigen is degenerated (Mason, 1998; Vrisekoop et al., 2014). Degenerate antigen recognition by TCR is an essential feature of T cell development since T cell progenitors are first positively selected on self-antigens in the thymus before they give rise to mature Tconvs that can then during infection react towards unrelated non-self antigens in the periphery. The degeneracy of T cell recognition is also important during heterologous immunity (Welsh and Selin, 2002). Such a high level of degeneracy has been proposed to be essential for limiting possible holes in the TCR repertoire and to ensure the robustness of T cell immunity (Anderton and Wraith, 2002; Mason, 1998; Sewell, 2012; Vrisekoop et al., 2014). A drawback of degeneracy is however the potential recognition of autoantigens, and consequently the risk of autoimmunity (Skowera et al., 2008, Wooldridge et al., 2012). In contrast, our data obtained with retrogenic mice highlighted that for some MOG-reactive TCR, the expression of MOG was critical for the development of Tregs. In this case the selecting peptide can also act as an agonist to stimulate the activation of MOG-reactive Tregs

in the periphery. Thus, some Tregs might follow the central dogma of the clonal selection theory, which proposes that an individual lymphocyte is specific for a single antigen (Jerne, 1955, 1971). It is possible that antigen recognition by Tregs is less degenerate than for Tconvs, and that the resulting holes in the regulatory repertoire are required to allow efficient immunity against non-self antigens. Our data indicate however that this mode of Treg development is not absolute. First, Tconv TCR allowed the development of low numbers of Tregs. Although these cells might provide little protection from CNS autoimmunity due to the low functional avidity of their TCR for MOG, they might recognize some foreign antigens with high affinity, which could explain the detection of Tregs reacting against microbial antigens in the naïve peripheral repertoire (Moon et al., 2011). Second, some of the four TCR cloned from MOG-reactive Tregs generated low levels of Tregs in the thymus of *Mog*-deficient retrogenic mice. Thus, in addition to the pathway of Treg development driven by endogenous antigen presentation in the thymus, other processes contribute in parallel to the generation of the peripheral Treg pool. This might explain why in a polyclonal repertoire deficiency in MOG expression resulted in an incomplete loss of thymic MOG-reactive Tregs compared to controls. It will be important to assess whether these different pathways of Treg development give rise to functionally distinct subsets. Our observation that in retrogenic mice the frequencies of cells expressing Helios vary in these distinct conditions suggests that these various Tregs are not identical.

The capacity of antigen(s) other than MOG to drive thymic selection of Tconvs more efficiently than Tregs suggests that these cells express TCR with different antigen-recognition properties. Our data obtained using a panel of altered peptides support the notion that the TCR from Tregs and Tconvs differentially interact with MOG. Some altered peptide ligands increased the amounts of IL-2 produced by the cell lines expressing Tconv-derived TCR by 2.7 to 10.1-fold compared to the original peptide, while the maximum increases observed for the Treg-derived TCR were lower (0.5 to 1.6-fold). This suggests that wild-type MOG is an optimal agonist for MOG-reactive Tregs but not for Tconvs. This might explain why MOG is so important for the development of MOG-reactive Tregs. Structural investigations will be necessary to precise how the TCR from Tregs and Tconvs recognize MOG. Structural characterization of two TCR carried by induced human regulatory T cells recently indicated that these TCR interacted differently with their antigen-MHC complex compared to previously characterized TCR-peptide-MHC complexes structures for Tconv TCR (Beringer et al., 2015).

Indirect evidence suggested that Treg development was favoured by TCR interactions of high functional avidity for the selecting antigens. This notion is however complicated to evaluate because antigen sensitivity is influenced by numerous parameters beyond the TCR identity, as shown by the fact that individual T cell clones can generate progeny with both high and low antigen sensitivity (Kroger and Alexander-Miller, 2007). Here, the identification of MOG as the cue controlling the differentiation of MOG-reactive Tregs enabled us to compare the characteristics distinguishing the

TCR implicated in the commitment of T cell progenitors into either Tregs or Tconvs. Our data confirmed that a major difference between these two types of TCR was their functional avidity for MOG, which was markedly higher for Tregs.

The expression by Tregs and Tconvs of TCR of different functional avidity for MOG led us to examine the relevance of this dichotomy for the function of these cells in the periphery. Polyclonal Tregs engineered to express a MOG-reactive Treg TCR almost completely prevented disease induction, while Tregs carrying Tconv TCR had only moderate to no protective value in EAE. Based on these observations, we propose that the expression of high performance TCR by Tregs is important for these cells to have a dominant effect over Tconvs for suppressing anti-self immunity.

There is currently intense interest in the possibility of using Tregs for the suppression of unwanted immunity in adoptive cell therapy. Several clinical trials have already been initiated to examine the safety and therapeutic value of polyclonal Tregs in the clinic (Brunstein et al., 2011; Di Ianni et al., 2011; Marek-Trzonkowska et al., 2012; Theil et al., 2015). Data obtained in pre-clinical models demonstrated that in autoimmune diseases, autoantigen-reactive Tregs were markedly superior to polyclonal Tregs to suppress pathology (Stephens et al., 2009). Thus, an attractive Treg-based strategy for treating autoimmune diseases would be to isolate a patient's own Tregs reacting against a disease-relevant autoantigen, expand them *ex vivo*, and subsequently use these cells in autologous adoptive cell therapy. However,

autoantigen-specific Tregs are rare and remain difficult to isolate making their application in adoptive cellular therapy challenging. The possibility of engineering Tregs by TCR gene transfer represents a major advance on this point, yet raises the new question about the choice of the type of TCR that should be used. Our data demonstrate that TCR from Tregs are clearly a preferable choice since they confer markedly superior protective functions to engineered Tregs than TCR from Tconvs.

In conclusion, we have demonstrated an unexpected role for endogenous MOG expression as a major cue for the selection of thymus-derived MOG-reactive Tregs, providing the first identification of a natural antigen that controls Treg differentiation. These results might help to understand how thymus-derived Tregs have a key role in preventing autoimmune-mediated attack of self-tissues, while allowing efficient defence against infections.

EXPERIMENTAL PROCEDURES

Detailed experimental procedures can be found in the Supplemental Information section.

Mice

Mouse strains are described in Supplemental Experimental Procedures. Experiments were performed in accordance with German, French, and U.K. authorities.

EAE induction through immunization and adoptive transfer

EAE was induced and assessed as described (Fillatreau et al., 2002). Some mice received 200 μg anti-CD25 (PC61) intravenously three days before EAE induction (Figure 1H). The protocol was in cases adjusted to use 5 μg of MOG(35-55) or 49(H_A) peptides (Figure 2D). Passive EAE was induced by adoptive transfer of activated Kaa T cells, or polyclonal Tconvs transduced to express a MOG-reactive TCR, as described in Supplemental Experimental Procedures.

Identification and cloning of Kaa TCRα chains

Kaa.Foxp3.IRES.eGFP^{+}TCR$\alpha^{+/-}$TCR$\beta^{+/-}$ mice were immunized with MOG(35-55) to induce EAE, and CD4^{+}GFP^{+} as well as CD4^{+}GFP^{-} cells were isolated from their CNS (brain and spinal cord) using a combination of magnetic and cytometric procedures. RNA was isolated from these cells using RNeasy mini Kit (Qiagen). cDNA was generated using a SMARTer 5' RACE cDNA Amplification Kit, and an Advantage 2 PCR Kit (both Clontech), using the

primer 5'-ACT GGA CCA CAG CCT CAG CGT CA-3'. PCR products were cloned into the pcDNA3.1/V5-His-TOPO vector (Life technologies). After transformation into *E. coli* positive colonies were sequenced (GATC Biotech). TCRα sequences were identified by IMGT HighV-quest software (www.imgt.org/HighV-QUEST) (Alamyar et al., 2012).

Expression of TCR in T.54ζ17 cells

T.54ζ17 cells (gift of B. Malissen, France) (Letourneur and Malissen, 1989), which express mouse CD4, were modified to stably express the Kaa TCRβ chain cloned into a pMig retroviral vector (Van Parijs et al., 1999). TCRα chains were cloned into the pMY-IRES-GFP retroviral vector (Cell Biolabs). T.54ζ17 cells expressing the Kaa TCRβ chain were transduced with pMY-IRES-GFP encoding the TCRα, and $GFP^{+}Vβ8.2^{+}$ cells were sorted on a FACSAria II several times until cultures stably containing >95% TCR-expressing cells were obtained. For each TCRα chain two TCR-expressing cell lines were independently generated.

Expression of TCR in HSC, Tconvs, and Tregs

The TCRα and Kaa TCRβ sequences were linked via a 2A element of porcine teschovirus (p2a) by PCR and cloned into the MP71 vector (Engels et al., 2003) via *Not*I and *Eco*RI restriction sites to obtain MP71-TCRβ-p2a-TCRα. The *Thy1.1* gene was additionally linked to the TCR chains using a 2A linker element of *Thosea asigna* virus (t2a) to yield MP71-TCRβ-p2a-TCRα-t2a-Thy1.1. To simultaneously express miRNAs in the MP71 vector, *Ctla4*-specific miRNA target sites GGT TCC AAA GGT TGT AGT GTT and AAC TGA AAG

GCC GTT TAT GAA were predicted by BLOCK-iT™ RNAi Designer (rnaidesigner.lifetechnologies.com/rnaiexpress) and the respective antisense sequences were integrated into two different miRNA environments (murine miR-155 (Chung et al., 2006) and an artificial miRNA (Saetrom et al., 2006)). Then, the miRNAs were inserted into the MP71 intron (Bunse et al., 2014). Other sequences and protocols for the utilization of these retroviral are described in Supplemental Experimental Procedures. TCR-retrogenic mice were prepared as described (Kieback et al., 2014).

Statistical analyses

Cumulative disease scores and data from peptide stimulations and TCR retrogenic mice were analyzed with an unpaired or paired two-tailed Student's t test. EAE disease courses were compared by repeated-measures two-way ANOVA. Statistical analysis was performed with GraphPad Prism (GraphPad Software Inc.). *P<0.05; **P<0.01; ***P< 0.001.

AUTHOR CONTRIBUTIONS

E.K., E.H., U.S., V.L., P.S., M.B., Y.J., P.B., A.R., U.K., A.A.K., R.L., N.H, S.M.A., W.U., and S.F. performed experiments, contributed to the development of the project, and to the writing of the manuscript.

ACKNOWLEDGEMENTS

We thank Carolin Genehr, Martina Kalupa, Christin Hesse, and Mareen Kamarys for technical help, Bernard Malissen for T.54ζ17 cells, Dimitris Kioussis (NIMR, UK) for the CD2 minigene expression system, and the NIH Tetramer Facility for the tetramers. This work was supported by the Deutsche Forschungsgemeinschaft (SFB-TR-36 and SFB-650).

REFERENCES

Alamyar, E., Duroux, P., Lefranc, M.P., and Giudicelli, V. (2012). IMGT((R)) tools for the nucleotide analysis of immunoglobulin (IG) and T cell receptor (TR) V-(D)-J repertoires, polymorphisms, and IG mutations: IMGT/V-QUEST and IMGT/HighV-QUEST for NGS. Methods in molecular biology *882*, 569-604.

Anderton, S.M., and Wraith, D.C. (2002). Selection and fine-tuning of the autoimmune T-cell repertoire. Nature reviews. Immunology *2*, 487-498.

Bautista, J.L., Lio, C.W., Lathrop, S.K., Forbush, K., Liang, Y., Luo, J., Rudensky, A.Y., and Hsieh, C.S. (2009). Intraclonal competition limits the fate determination of regulatory T cells in the thymus. Nature immunology *10*, 610-617.

Bennett, C.L., Christie, J., Ramsdell, F., Brunkow, M.E., Ferguson, P.J., Whitesell, L., Kelly, T.E., Saulsbury, F.T., Chance, P.F., and Ochs, H.D. (2001). The immune dysregulation, polyendocrinopathy, enteropathy, X-linked syndrome (IPEX) is caused by mutations of FOXP3. Nature genetics *27*, 20-21.

Beringer, D.X., Kleijwegt, F.S., Wiede, F., van der Slik, A.R., Loh, K.L., Petersen, J., Dudek, N.L., Duinkerken, G., Laban, S., Joosten, A.*, et al.* (2015). T cell receptor reversed polarity recognition of a self-antigen major histocompatibility complex. Nature immunology *16*, 1153-1161.

Brunstein, C.G., Miller, J.S., Cao, Q., McKenna, D.H., Hippen, K.L., Curtsinger, J., Defor, T., Levine, B.L., June, C.H., Rubinstein, P.*, et al.* (2011). Infusion of ex vivo expanded T regulatory cells in adults transplanted with

umbilical cord blood: safety profile and detection kinetics. Blood *117*, 1061-1070.

Bunse, M., Bendle, G.M., Linnemann, C., Bies, L., Schulz, S., Schumacher, T.N., and Uckert, W. (2014). RNAi-mediated TCR knockdown prevents autoimmunity in mice caused by mixed TCR dimers following TCR gene transfer. Molecular therapy : the journal of the American Society of Gene Therapy *22*, 1983-1991.

Chinen, T., Volchkov, P.Y., Chervonsky, A.V., and Rudensky, A.Y. (2010). A critical role for regulatory T cell-mediated control of inflammation in the absence of commensal microbiota. The Journal of experimental medicine *207*, 2323-2330.

Chung, K.H., Hart, C.C., Al-Bassam, S., Avery, A., Taylor, J., Patel, P.D., Vojtek, A.B., and Turner, D.L. (2006). Polycistronic RNA polymerase II expression vectors for RNA interference based on BIC/miR-155. Nucleic acids research *34*, e53.

Di Ianni, M., Falzetti, F., Carotti, A., Terenzi, A., Castellino, F., Bonifacio, E., Del Papa, B., Zei, T., Ostini, R.I., Cecchini, D.*, et al.* (2011). Tregs prevent GVHD and promote immune reconstitution in HLA-haploidentical transplantation. Blood *117*, 3921-3928.

Engels, B., Cam, H., Schuler, T., Indraccolo, S., Gladow, M., Baum, C., Blankenstein, T., and Uckert, W. (2003). Retroviral vectors for high-level transgene expression in T lymphocytes. Human gene therapy *14*, 1155-1168.

Fazilleau, N., Delarasse, C., Sweenie, C.H., Anderton, S.M., Fillatreau, S., Lemonnier, F.A., Pham-Dinh, D., and Kanellopoulos, J.M. (2006). Persistence of autoreactive myelin oligodendrocyte glycoprotein (MOG)-specific T cell

repertoires in MOG-expressing mice. European journal of immunology *36*, 533-543.

Fillatreau, S., Sweenie, C.H., McGeachy, M.J., Gray, D., and Anderton, S.M. (2002). B cells regulate autoimmunity by provision of IL-10. Nature immunology *3*, 944-950.

Fontenot, J.D., Gavin, M.A., and Rudensky, A.Y. (2003). Foxp3 programs the development and function of CD4+CD25+ regulatory T cells. Nature immunology *4*, 330-336.

Frentsch, M., Arbach, O., Kirchhoff, D., Moewes, B., Worm, M., Rothe, M., Scheffold, A., and Thiel, A. (2005). Direct access to CD4+ T cells specific for defined antigens according to CD154 expression. Nature medicine *11*, 1118-1124.

Hovelmeyer, N., Hao, Z., Kranidioti, K., Kassiotis, G., Buch, T., Frommer, F., von Hoch, L., Kramer, D., Minichiello, L., Kollias, G*., et al.* (2005). Apoptosis of oligodendrocytes via Fas and TNF-R1 is a key event in the induction of experimental autoimmune encephalomyelitis. Journal of immunology *175*, 5875-5884.

Hsieh, C.S., Zheng, Y., Liang, Y., Fontenot, J.D., and Rudensky, A.Y. (2006). An intersection between the self-reactive regulatory and nonregulatory T cell receptor repertoires. Nature immunology *7*, 401-410.

Jerne, N.K. (1955). The Natural-Selection Theory of Antibody Formation. Proceedings of the National Academy of Sciences of the United States of America *41*, 849-857.

Jerne, N.K. (1971). The somatic generation of immune recognition. European journal of immunology *1*, 1-9.

Jordan, M.S., Boesteanu, A., Reed, A.J., Petrone, A.L., Holenbeck, A.E., Lerman, M.A., Naji, A., and Caton, A.J. (2001). Thymic selection of CD4+CD25+ regulatory T cells induced by an agonist self-peptide. Nature immunology *2*, 301-306.

Kieback, E., Hilgenberg, E., and Fillatreau, S. (2014). A method for the generation of TCR retrogenic mice. Methods in molecular biology *1193*, 117-126.

Kroger, C.J., and Alexander-Miller, M.A. (2007). Cutting edge: CD8+ T cell clones possess the potential to differentiate into both high- and low-avidity effector cells. Journal of immunology *179*, 748-751.

Letourneur, F., and Malissen, B. (1989). Derivation of a T cell hybridoma variant deprived of functional T cell receptor alpha and beta chain transcripts reveals a nonfunctional alpha-mRNA of BW5147 origin. European journal of immunology *19*, 2269-2274.

Leung, M.W., Shen, S., and Lafaille, J.J. (2009). TCR-dependent differentiation of thymic Foxp3+ cells is limited to small clonal sizes. The Journal of experimental medicine *206*, 2121-2130.

Levine, A.G., Arvey, A., Jin, W., and Rudensky, A.Y. (2014). Continuous requirement for the TCR in regulatory T cell function. Nature immunology *15*, 1070-1078.

Mahmud, S.A., Manlove, L.S., Schmitz, H.M., Xing, Y., Wang, Y., Owen, D.L., Schenkel, J.M., Boomer, J.S., Green, J.M., Yagita, H.*, et al.* (2014). Costimulation via the tumor-necrosis factor receptor superfamily couples TCR signal strength to the thymic differentiation of regulatory T cells. Nature immunology *15*, 473-481.

Marek-Trzonkowska, N., Mysliwiec, M., Dobyszuk, A., Grabowska, M., Techmanska, I., Juscinska, J., Wujtewicz, M.A., Witkowski, P., Mlynarski, W., Balcerska, A.*, et al.* (2012). Administration of CD4+CD25highCD127-regulatory T cells preserves beta-cell function in type 1 diabetes in children. Diabetes care *35*, 1817-1820.

Mason, D. (1998). A very high level of crossreactivity is an essential feature of the T-cell receptor. Immunology today *19*, 395-404.

McGeachy, M.J., Stephens, L.A., and Anderton, S.M. (2005). Natural recovery and protection from autoimmune encephalomyelitis: contribution of CD4+CD25+ regulatory cells within the central nervous system. Journal of immunology *175*, 3025-3032.

Moon, J.J., Dash, P., Oguin, T.H., 3rd, McClaren, J.L., Chu, H.H., Thomas, P.G., and Jenkins, M.K. (2011). Quantitative impact of thymic selection on Foxp3+ and Foxp3- subsets of self-peptide/MHC class II-specific CD4+ T cells. Proceedings of the National Academy of Sciences of the United States of America *108*, 14602-14607.

Moran, A.E., Holzapfel, K.L., Xing, Y., Cunningham, N.R., Maltzman, J.S., Punt, J., and Hogquist, K.A. (2011). T cell receptor signal strength in Treg and iNKT cell development demonstrated by a novel fluorescent reporter mouse. The Journal of experimental medicine *208*, 1279-1289.

Morikawa, H., and Sakaguchi, S. (2014). Genetic and epigenetic basis of Treg cell development and function: from a FoxP3-centered view to an epigenome-defined view of natural Treg cells. Immunological reviews *259*, 192-205.

Pacholczyk, R., Ignatowicz, H., Kraj, P., and Ignatowicz, L. (2006). Origin and T cell receptor diversity of Foxp3+CD4+CD25+ T cells. Immunity *25*, 249-259.

Pacholczyk, R., Kern, J., Singh, N., Iwashima, M., Kraj, P., and Ignatowicz, L. (2007). Nonself-antigens are the cognate specificities of Foxp3+ regulatory T cells. Immunity *27*, 493-504.

Pennington, D.J., Silva-Santos, B., Silberzahn, T., Escorcio-Correia, M., Woodward, M.J., Roberts, S.J., Smith, A.L., Dyson, P.J., and Hayday, A.C. (2006). Early events in the thymus affect the balance of effector and regulatory T cells. Nature *444*, 1073-1077.

Saetrom, P., Snove, O., Nedland, M., Grunfeld, T.B., Lin, Y., Bass, M.B., and Canon, J.R. (2006). Conserved microRNA characteristics in mammals. Oligonucleotides *16*, 115-144.

Sewell, A.K. (2012). Why must T cells be cross-reactive? Nature reviews. Immunology *12*, 669-677.

Skowera, A., Ellis, R.J., Varela-Calvino, R., Arif, S., Huang, G.C., Van-Krinks, C., Zaremba, A., Rackham, C., Allen, J.S., Tree, T.I.*, et al.* (2008). CTLs are targeted to kill beta cells in patients with type 1 diabetes through recognition of a glucose-regulated preproinsulin epitope. The Journal of clinical investigation *118*, 3390-3402.

Stephens, L.A., Malpass, K.H., and Anderton, S.M. (2009). Curing CNS autoimmune disease with myelin-reactive Foxp3+ Treg. European journal of immunology *39*, 1108-1117.

Theil, A., Tuve, S., Oelschlagel, U., Maiwald, A., Dohler, D., Ossmann, D., Zenkel, A., Wilhelm, C., Middeke, J.M., Shayegi, N.*, et al.* (2015). Adoptive transfer of allogeneic regulatory T cells into patients with chronic graft-versus-host disease. Cytotherapy *17*, 473-486.

Thornton, A.M., Korty, P.E., Tran, D.Q., Wohlfert, E.A., Murray, P.E., Belkaid, Y., and Shevach, E.M. (2010). Expression of Helios, an Ikaros transcription factor family member, differentiates thymic-derived from peripherally induced Foxp3+ T regulatory cells. Journal of immunology *184*, 3433-3441.

van den Elzen, P., Menezes, J.S., Ametani, A., Maverakis, E., Madakamutil, L., Tang, X.L., Kumar, V., and Sercarz, E.E. (2004). Limited clonality in autoimmunity: drivers and regulators. Autoimmunity reviews *3*, 524-529.

Van Parijs, L., Refaeli, Y., Lord, J.D., Nelson, B.H., Abbas, A.K., and Baltimore, D. (1999). Uncoupling IL-2 signals that regulate T cell proliferation, survival, and Fas-mediated activation-induced cell death. Immunity *11*, 281-288.

van Santen, H.M., Benoist, C., and Mathis, D. (2004). Number of T reg cells that differentiate does not increase upon encounter of agonist ligand on thymic epithelial cells. The Journal of experimental medicine *200*, 1221-1230.

Verhagen, J., Gabrysova, L., Minaee, S., Sabatos, C.A., Anderson, G., Sharpe, A.H., and Wraith, D.C. (2009). Enhanced selection of FoxP3+ T-regulatory cells protects CTLA-4-deficient mice from CNS autoimmune disease. Proceedings of the National Academy of Sciences of the United States of America *106*, 3306-3311.

Vrisekoop, N., Monteiro, J.P., Mandl, J.N., and Germain, R.N. (2014). Revisiting thymic positive selection and the mature T cell repertoire for antigen. Immunity *41*, 181-190.

Welsh, R.M., and Selin, L.K. (2002). No one is naive: the significance of heterologous T-cell immunity. Nature reviews. Immunology *2*, 417-426.

Wing, K., Onishi, Y., Prieto-Martin, P., Yamaguchi, T., Miyara, M., Fehervari, Z., Nomura, T., and Sakaguchi, S. (2008). CTLA-4 control over Foxp3+ regulatory T cell function. Science *322*, 271-275.

Wooldridge, L., Ekeruche-Makinde, J., van den Berg, H.A., Skowera, A., Miles, J.J., Tan, M.P., Dolton, G., Clement, M., Llewellyn-Lacey, S., Price, D.A.*, et al.* (2012). A single autoimmune T cell receptor recognizes more than a million different peptides. The Journal of biological chemistry *287*, 1168-1177.

Yednock, T.A., Cannon, C., Fritz, L.C., Sanchez-Madrid, F., Steinman, L., and Karin, N. (1992). Prevention of experimental autoimmune encephalomyelitis by antibodies against alpha 4 beta 1 integrin. Nature *356*, 63-66.

FIGURE LEGENDS

Figure 1. The Kaa mouse

A. LN cells isolated from Kaa mice on day 8 post-immunization with MOG(35-55) were re-stimulated with MOG(35-55) for 3 days, and (left panel) analysed by flow cytometry to quantify cytokine-expressing $CD4^+$ T cells, or (right panel) adoptively transferred in recipient mice. Data show mean EAE score ± sem from a pool of two experiments (n=12). **B**. Cells from LN and spleens from naïve Kaa or C57BL/6 mice were depleted from $CD25^+$ cells, and stimulated with MOG(35-55) for 3 days *in vitro*, prior to analysis by flow cytometry (left, only Kaa) or adoptive transfer (right). Pooled data (mean EAE score ± sem) from three experiments (C57BL/6: n=10, Kaa: n=13). **C**. EAE was induced in Kaa (n=12) and C57BL/6 (n=6) mice by immunization with MOG(35-55). Data show mean EAE score + sem. **D.** LN cells of Kaa.Foxp3.eGFP (Kaa, n=4) or Foxp3.eGFP (B6, n=2) mice were stained with MOG-I-A(b)-PE and control-I-A(b)-APC tetramers. Data show frequency of MOG-I-A(b)-binding cells in Tregs and Tconvs (left, pooled results from all mice) and representative stainings (right) gated on $CD4^+GFP^+$ cells for Kaa.Foxp3.eGFP (Kaa Treg) and Foxp3.eGFP (B6 Treg) mice. **E.** Splenocytes from naïve Kaa mice were depleted or not of CD25-expressing cells, and stimulated for 72 h with MOG(35-55) to measure their proliferation by ^{3}H-thymidine incorporation. Data show mean values of triplicates. Representative results from one of two experiments. **F.** EAE course of C57BL/6 mice that received Tregs from naïve Kaa (n=12) or C57BL/6 (n=13) mice or PBS (n=13) on day 1 before EAE induction by immunization with MOG(35-55). Data show results (mean EAE score + sem) pooled from three

experiments. Statistic was calculated comparing B6 Treg vs. Kaa Treg. **G.** Tregs from Kaa or C57BL/6 mice were labelled with Cell Proliferation Dye eFluor450 and injected into CD45.1$^+$ C57BL/6 mice. Mice were immunized with either MOG(35-55) or OVA(323-369) and the number of CD45.2$^+$CD4$^+$Foxp3$^+$ cells in the draining LN was determined six days later. Data pooled from two experiments (n=9 per group). **H.** Kaa mice were treated with anti-CD25 (PC61) (n=11) or left untreated (n=10) and immunized with MOG(35-55) to induce EAE. Data show results (mean EAE score + sem) pooled from two experiments. See also Figure S1.

Figure 2. Antigen recognition properties of TCR from MOG-reactive Tregs and Tconvs

A. Relative frequencies of the selected TCRα among the total number of sequences analysed for Tregs (grey) and Tconvs (white). Each segment within a bar corresponds to one of the three independent experiments. Relative frequencies were calculated by dividing the counts of each selected sequence per experiment by the total number of sequences analysed in this experiment. The indexes “T” and “N” indicate sequences found in the three Tregs and Tconvs samplings, respectively. **B.** The T.54ζ17 cell lines expressing MOG-reactive TCR from Tregs (n=17) or Tconvs (n=11) were stimulated with MOG(35-55) in indicated concentrations, and IL-2 production was quantified by ELISA. Data show one representative of three experiments. **C.** The cell lines used in B (Tregs: n=17, Tconvs: n=11) were stimulated with MOG(35-55) peptide variants or WT MOG(35-55). Data show the change in IL-2 produced after stimulation with each variant peptide relatively to WT

MOG(35-55). One representative of two experiments. **D.** Kaa mice were immunized with 49(H_A) or MOG(35-55). Data show mean EAE score + sem, and are pooled from two experiments (n=12). **E.** Blood was collected from mice shown in D on day 10 after immunization, and re-stimulated for 5 h with MOG(35-55) *ex vivo* to quantify CD40L- and cytokine-expressing $CD4^+$ T cells. Shown are mean + sem. See also Figure S2 and Table S1.

Figure 3. Role of TCR for Treg development

HSC from $CD45.2^+Rag^{-/-}$ mice were transduced with one of 12 MOG-reactive TCR and used to reconstitute $CD45.1^+$ C57BL/6 mice. **A.** Donor-derived $CD45.2^+CD4^+$ T cells were quantified in blood. **B.** Blood lymphocytes were analysed for the percentage of $Foxp3^+$ cells among donor-derived $CD45.2^+CD4^+$ cells. C57BL/6 mice were included as control. **C.** Thymus and spleen of retrogenic mice were analysed for percentages of $Foxp3^+$ cells among donor-derived $CD45.2^+CD4^+CD8^-$ T cells (upper panels) and absolute numbers (lower panels) of $CD45.2^+CD4^+CD8^-Foxp3^+$ cells 9 weeks after reconstitution. **D.** Expression of Helios in donor-derived $CD45.2^+CD4^+CD8^-$ $Foxp3^+$ Tregs in thymus and spleen. **A.-D.** Data (mean + sem) show pool from two experiments (n=9/10 mice per TCR) and are analysed comparing all mice prepared with Tconv TCR vs. all mice made with Treg TCR (unpaired t-test). See also Figure S3.

Figure 4. Role of MOG for the development of MOG-reactive Tregs. A.-C. HSC of $CD45.1^+Rag^{-/-}$ mice were transduced with one of four MOG-reactive TCR from Tregs, and used to reconstitute C57BL/6 (black bars) or $MOG^{-/-}$

(white bars) mice. Nine weeks later, thymus, spleen, and LN were analysed. WT C57BL/6 (grey bars) were included as control. **A. and B.** Percentage of $Foxp3^+$ cells among donor-derived $CD45.1^+CD4^+$ cells, and absolute numbers of $CD45.1^+CD4^+Foxp3^+$ Tregs. **C**. Frequency of Helios-expressing cells in $CD45.1^+CD4^+Foxp3^+$ Tregs. **A.-C.** Data pooled from two experiments (n=9/10 mice per TCR). **D. and E.** C57BL/6 (black bars, n=8) and $MOG^{-/-}$ (white bars, n=7) mice were reconstituted with CD90-depleted bone marrow cells from Kaa.Foxp3.eGFP mice. Thymocytes were analysed 5 weeks later by flow cytometry after staining with MOG-I-A(b) tetramer and αCD4. Data show percentage of MOG-I-A(b)-binding cells among $CD4^+CD8^-GFP^+$ Tregs, and absolute numbers of MOG-I-A(b)-binding $CD4^+CD8^-GFP^+$ Tregs. Representative stainings show MOG-I-A(b) and control-I-A(b) tetramer staining gated on live thymic donor-derived $CD4^+CD8^-GFP^+$ Tregs in C57BL/6 and $MOG^{-/-}$ recipients. **E.** Absolute numbers of MOG-I-A(b)$^+CD4^+CD8^-GFP^-$ T cells in thymus of reconstituted C57BL/6 and $MOG^{-/-}$ mice analysed in D. Data show mean + sem, and are pooled from two experiments. See also Figure S4.

Figure 5. TCR functional affinity determines the function of MOG-reactive Tregs and Tconvs

A. Polyclonal Tconvs were activated and transduced with retroviral vectors encoding for one of four MOG-reactive TCR and the marker Thy1.1. FACS plots show expression of Thy1.1 by T cells two days after transduction. Numbers indicate the percentage of $Thy1.1^+CD4^+$ cells among lymphocytes in the culture. **B.** TCR-modified Tconvs obtained as in A were stimulated for 24 h with MOG(35-55) in the presence of irradiated splenocytes. IFN-γ

concentration in supernatant was measured by ELISA. Data show means + sem of duplicates. One representative of two experiments. Statistics were calculated comparing all values from Tconv TCR vs. all values from Treg TCR for each peptide concentration. **C. and D.** TCR-modified Tconvs obtained as in A were used to induce EAE in recipient C57BL/6 mice via adoptive transfer. **C.** Seven days after transfer the percentage of Thy1.1$^+$ cells among peripheral blood CD4$^+$ T cells was determined. **D.** Data show mean EAE score + sem. Data in (C) and (D) are pooled from two experiments (n=10 per group). Statistics were calculated comparing the EAE curves from all mice receiving Tconv TCR vs. those from mice receiving Treg TCR. **E.** Polyclonal Tregs from C57BL/6 mice were activated and transduced with retroviral vectors encoding for one of the four different MOG-reactive TCR and Thy1.1. FACS plots show expression of Foxp3 and Thy1.1 by CD4$^+$ T cells on day two after transduction. Numbers indicate the percentage of Thy1.1$^+$Foxp3$^+$ cells among CD4$^+$ T cells. **F.** TCR-engineered Tregs produced as in E, or PBS, were administered to C57BL/6 mice one day before EAE induction by immunization with MOG(35-55). Data show mean EAE score + sem, and are pooled from three experiments (n=9 to 15 per group). Statistics were calculated comparing the EAE curves from all mice receiving Tconv TCR vs. those from mice receiving Treg TCR. **G.** Blood samples of mice from F were collected on day 10 after immunization, re-stimulated with MOG(35-55) for 5 h, and analysed by flow cytometry to quantify the frequency of CD4$^+$ T cells expressing CD40L, IFN-γ, or IL-17A. Graphs show mean ± sem, and are pooled from two experiments (n=5 to 10 per group). See also Figure S5.

Figure 6. Protective function of engineered MOG-reactive Tregs

A. and B. C57BL/6 mice were treated with PBS, or engineered Tregs expressing the TCR T6-106 and Thy1.1, or a mock vector coding only for Thy1.1, and immunized with MOG(35-55) one day post-transfer to induce EAE. **A.** On day 9 post-immunization, draining LN (popliteal and inguinal) cells from 5 mice were pooled and re-stimulated *in vitro* for 6 h with MOG(35-55), and analysed for intracellular cytokines and CD40L expression by flow cytometry. One representative of two experiments. **B.** CNS (brain plus spinal cord) from 5 mice were pooled and analysed at indicated days after EAE induction by flow cytometry. One representative of two experiments. **C.** C57BL/6 mice were immunized with MOG(35-55) and treated 8 days later with $2x10^6$ T6-106 TCR-transduced Tregs or PBS. Data show mean EAE score + sem, and cumulative disease scores (pooled from three experiments with n=14/15 per group). **D.** C57BL/6 mice received $2x10^6$ T6-106 TCR-transduced Tregs or PBS, and were immunized 6 weeks later with MOG(35-55) to induce EAE. Data show mean EAE score + sem, and cumulative disease scores (pool from two experiments with n=10/14 per group). See also Figure S6.

Figure 7. CTLA-4 controls protection from EAE by engineered Tregs

A. Design of the retroviral vector coding for T6-106 TCR, Thy1.1, and two intronic miRNAs**. B.** Polyclonal Tregs were activated and transduced with a vector as in A harbouring *Ctla-4*-, *Cd49d*- or *Tnfrsf18*- (GITR) specific miRNAs, or control miRNAs, and analysed two days post-transduction for CTLA-4, CD49d or GITR expression, respectively. Plots are gated on $Foxp3^+$

cells. One representative of three experiments. **C.** C57BL/6 mice were treated with $2x10^5$ Tregs transduced as in B, and immunized one day later with MOG(35-55). Data show mean EAE score + sem (pool from two experiments, n=10 per group). **D.** Mice treated with transduced CTLA-4-silenced Tregs, and immunised with MOG(35-55) as in C were analysed on day 13 post-immunization by flow cytometry to measure expression levels of CTLA-4 in the administered transduced $CD45.2^+Thy1.1^+CD4^+Foxp3^+$Tregs (n=5) in spleen. **E.** Absolute numbers of administered transduced $Thy1.1^+Foxp3^+$ Tregs in spleen of mice from D (pool of 2 experiments, n=10 per group).

Figure 1

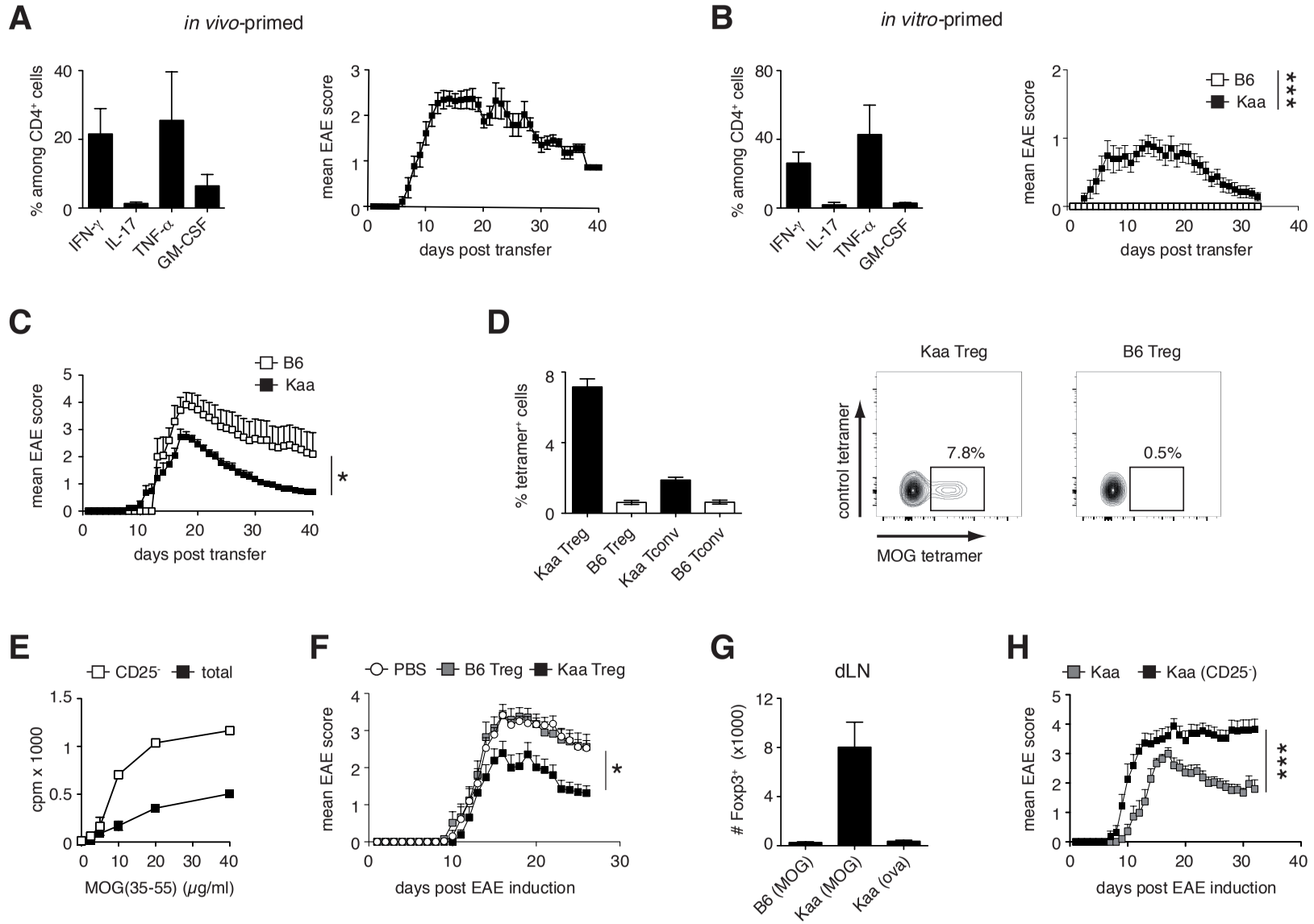

Figure 1

Figure 2

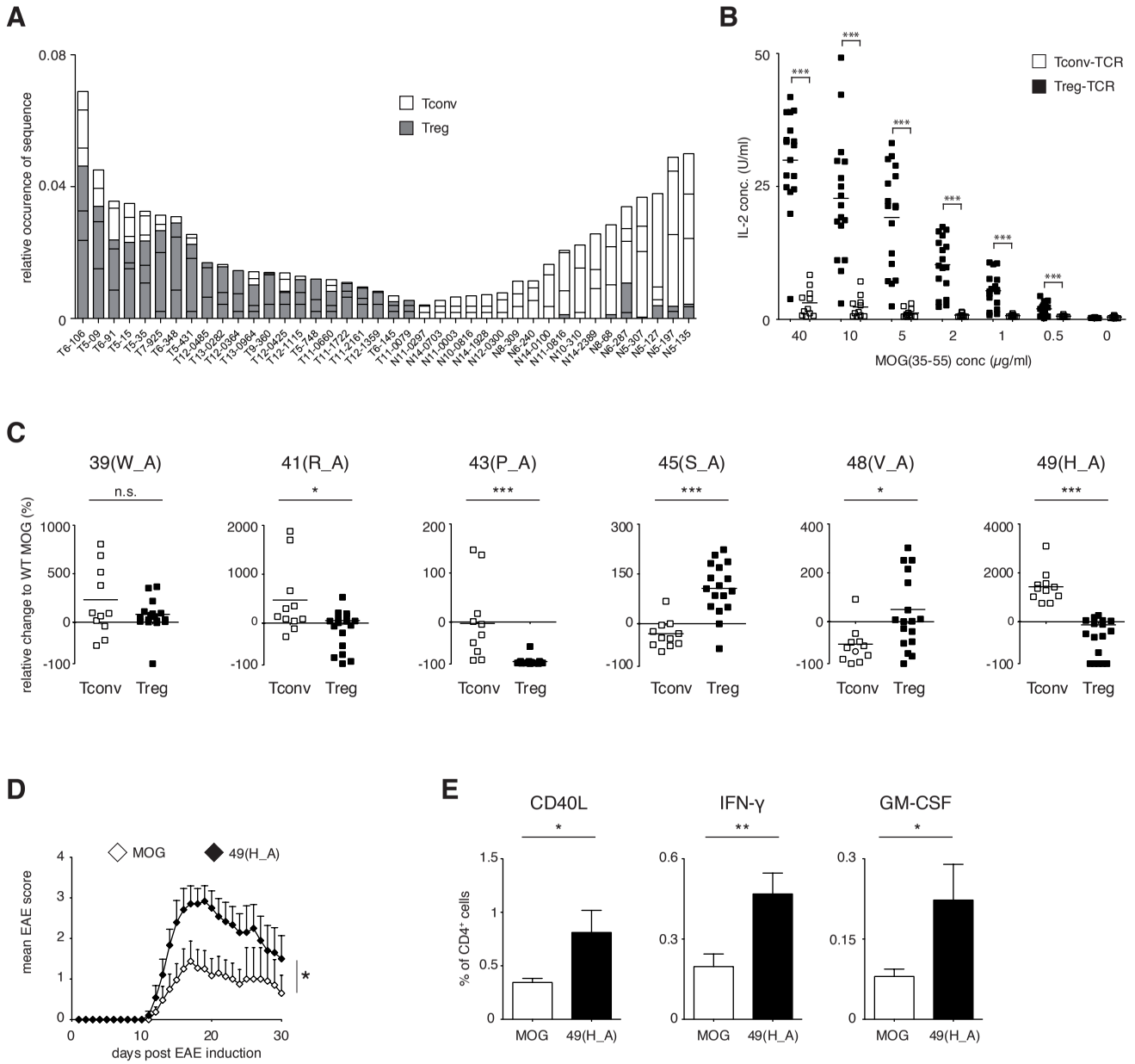

Figure 2

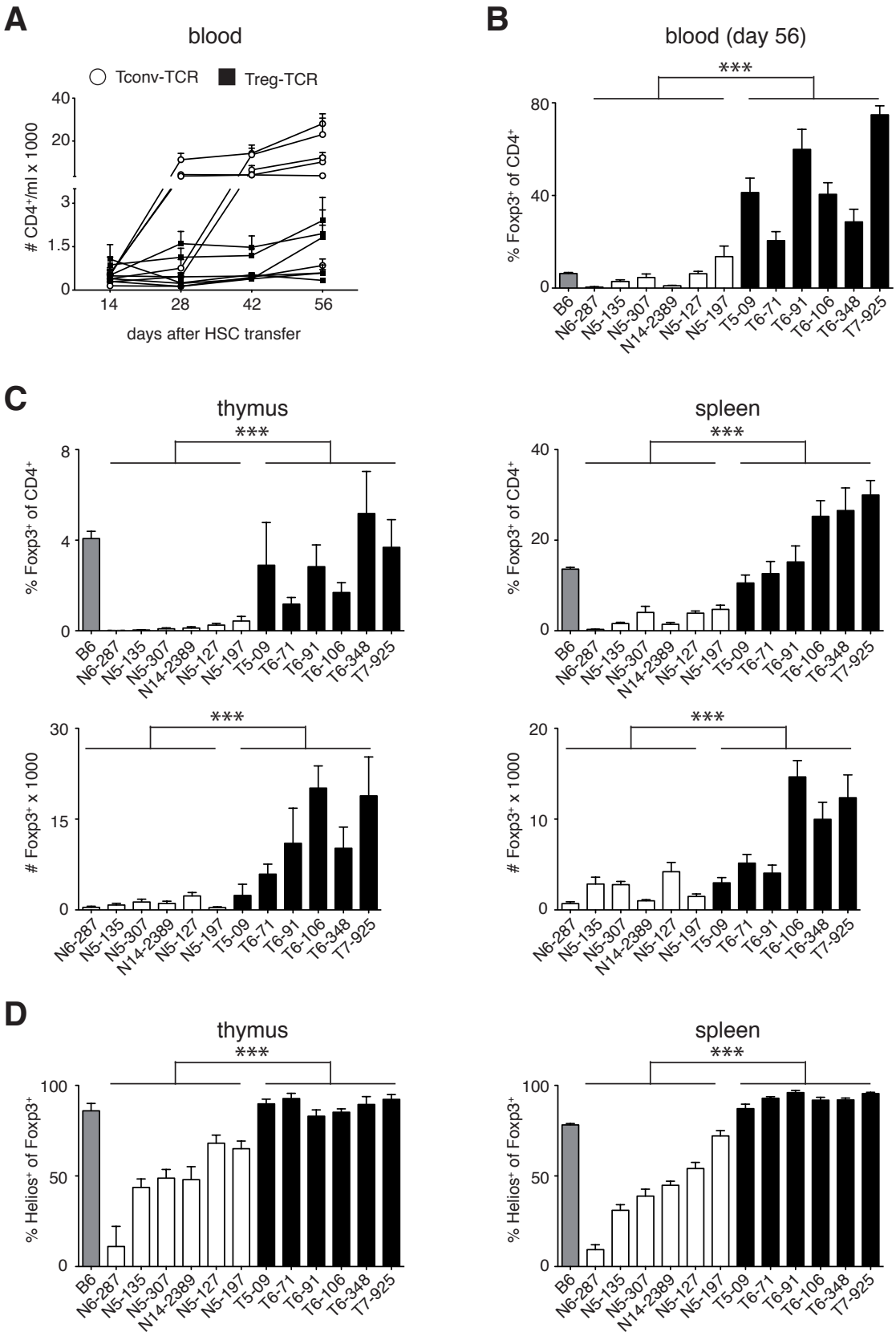
A
blood
Tconv-TCR
Treg-TCR
CD4+/ml x 1000
days after HSC transfer
B
blood (day 56)
% Foxp3+ of CD4+
C
thymus
spleen
% Foxp3+ of CD4+
# Foxp3+ x 1000
D
% Helios+ of Foxp3+
***
B6
N6-287
N5-135
N5-307
N14-2389
N5-127
N5-197
T5-09
T6-71
T6-91
T6-106
T6-348
T7-925

Figure 3

Figure 4

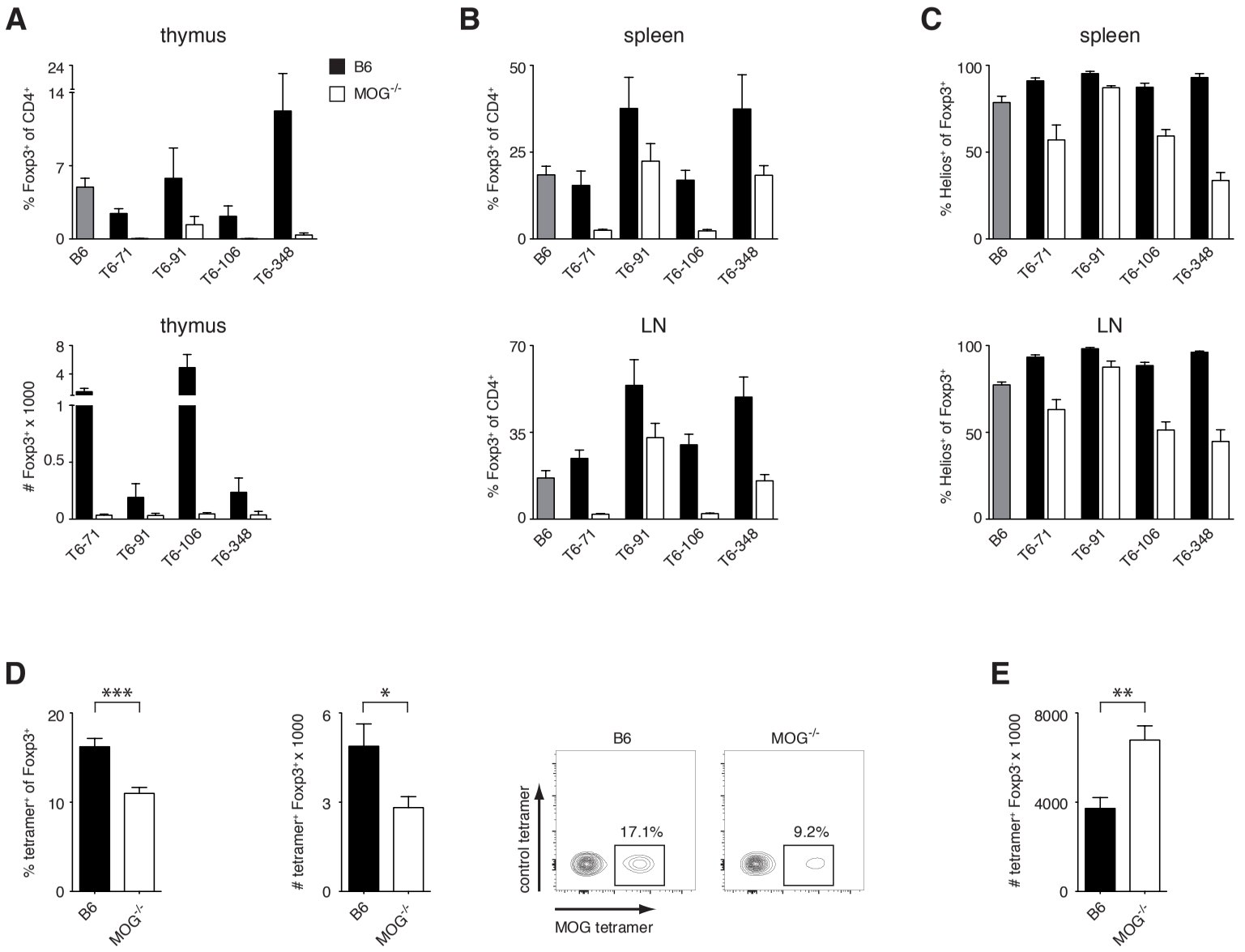

Figure 4

Figure 5

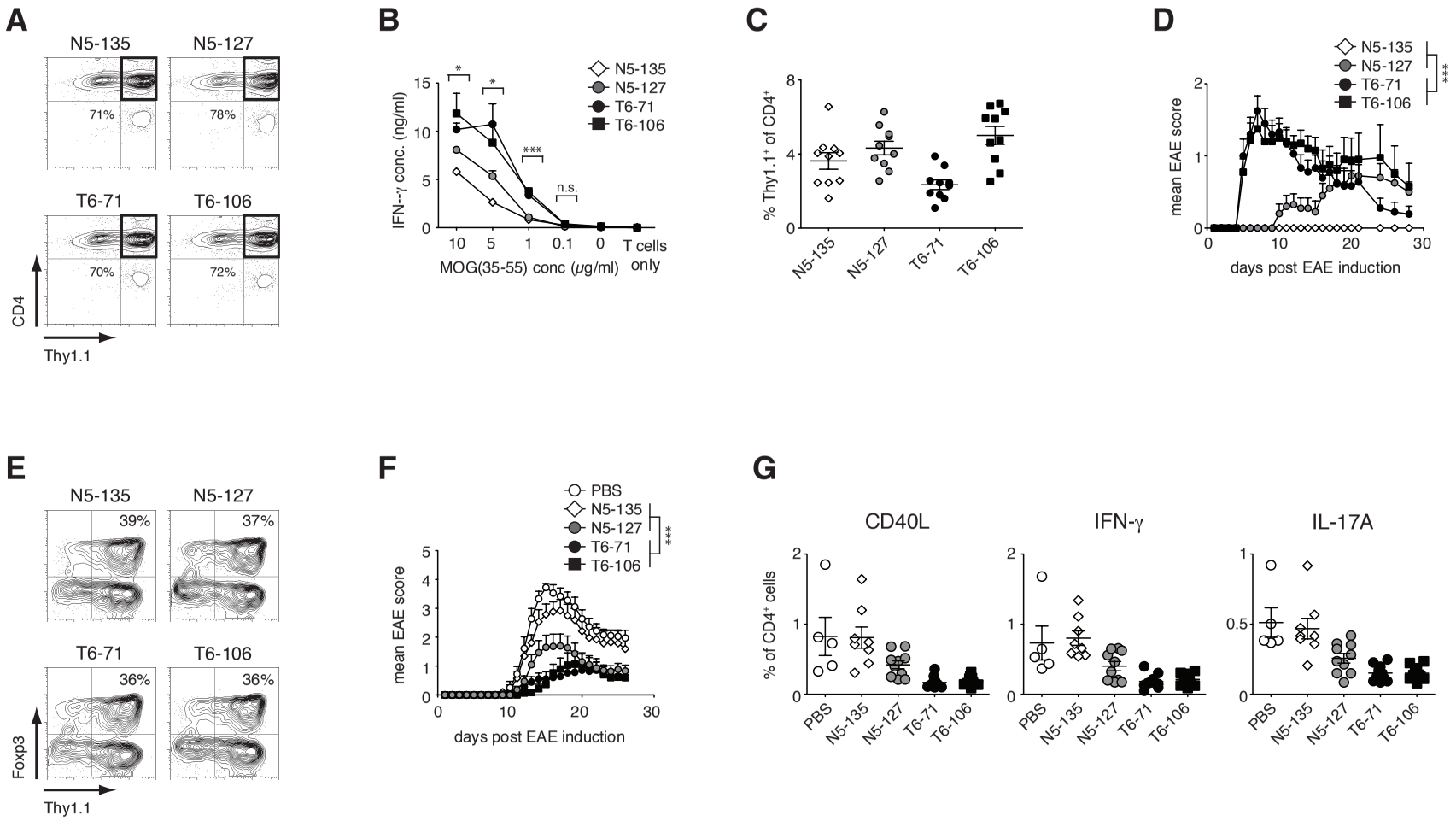

Figure 5

Figure 6

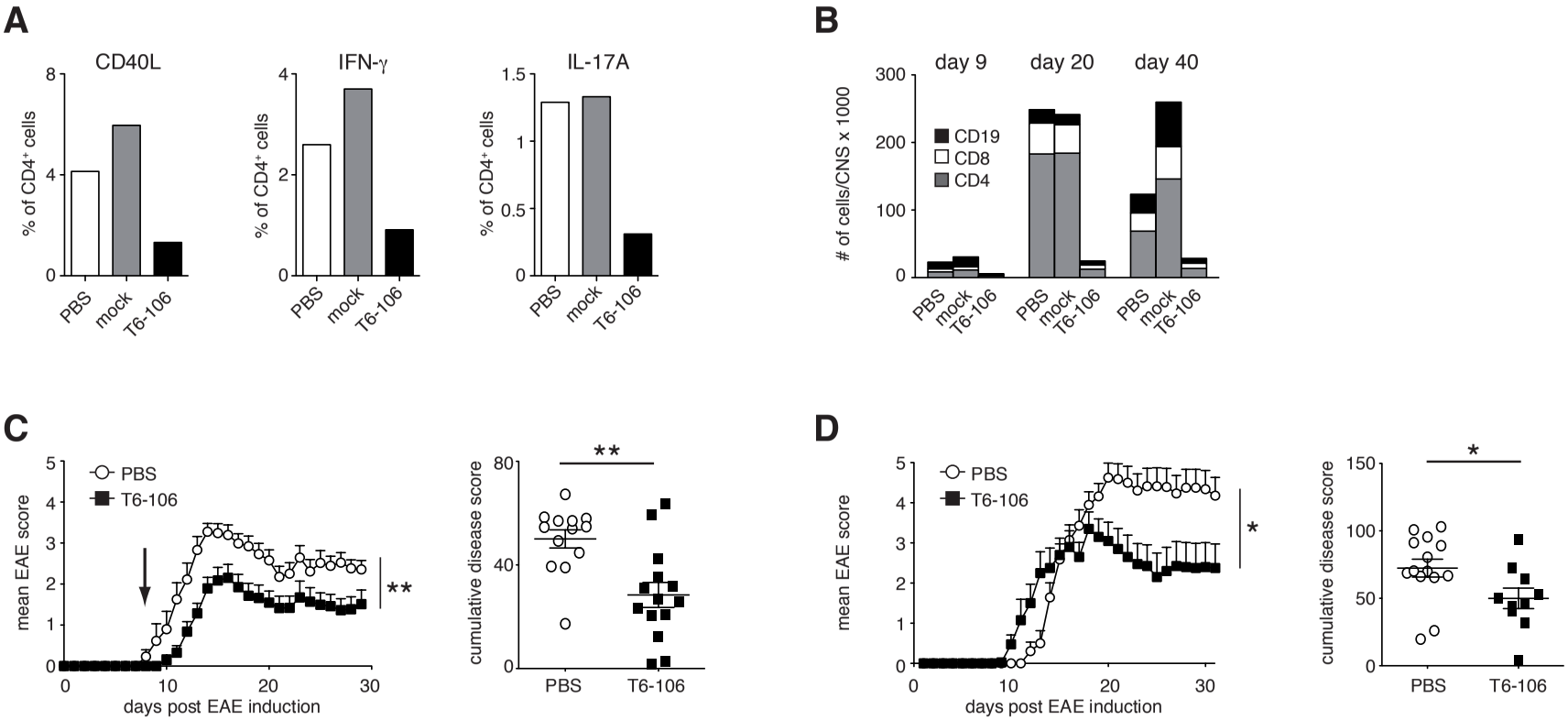

Figure 6

Figure 7

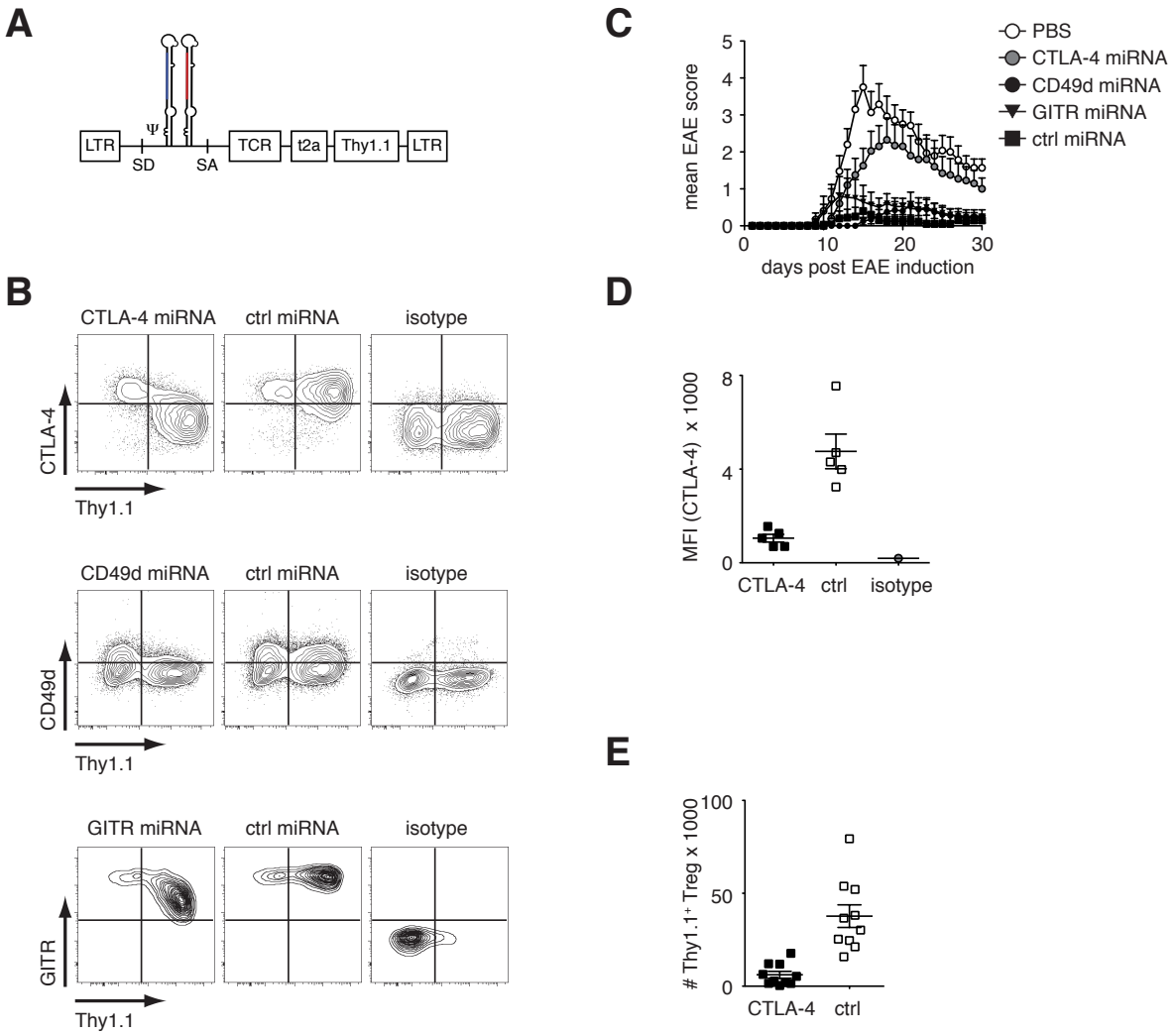

Figure 7

Supplemental figures and legends

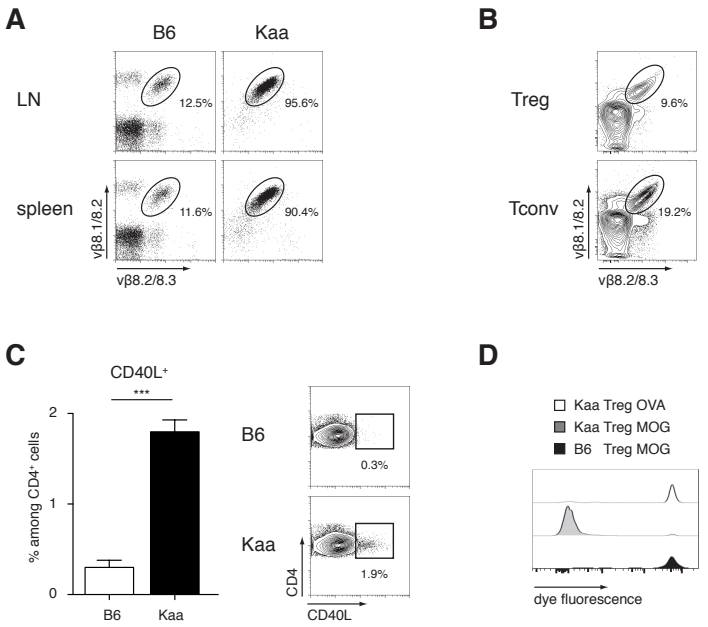

Figure S1, related to Figure 1 | Kaa: A transgenic mouse with increased frequencies of MOG-reactive protective Tregs and pathogenic Tconvs.

A. Representative FACS plots of Vβ8.2$^+$ cells among CD3$^+$ cells in LN and spleen of naïve Kaa and C57BL/6 (B6) mice. **B.** Representative FACS plots showing Vβ8.2$^+$ cells among CD4$^+$Foxp3$^+$ Tregs and CD4$^+$Foxp3$^-$ Tconvs in the CNS of C57BL/6 mice on day 40 after EAE induction. **C.** Frequency of CD40L$^+$ cells among CD4$^+$ T cells in spleen from naïve Kaa (n=5) and C57BL/6 (n=3) mice after *in vitro* stimulation with MOG(35-55) for 5 h. FACS plots are gated on CD4$^+$ T cells. Representative results of more than three experiments. **D.** Tregs from Kaa or C57BL/6 mice were labelled with eFluor450 dye, and injected into CD45.1$^+$ C57BL/6 mice that were subsequently immunized with either MOG(35-55) (MOG) or OVA(323-339) (OVA) peptides in CFA, as indicated. The histogram shows a representative staining of eFluor450 dye dilution in the transferred CD45.2$^+$CD4$^+$Foxp3$^+$ Kaa and C57BL/6 cells in the draining LN six days after transfer and immunization.

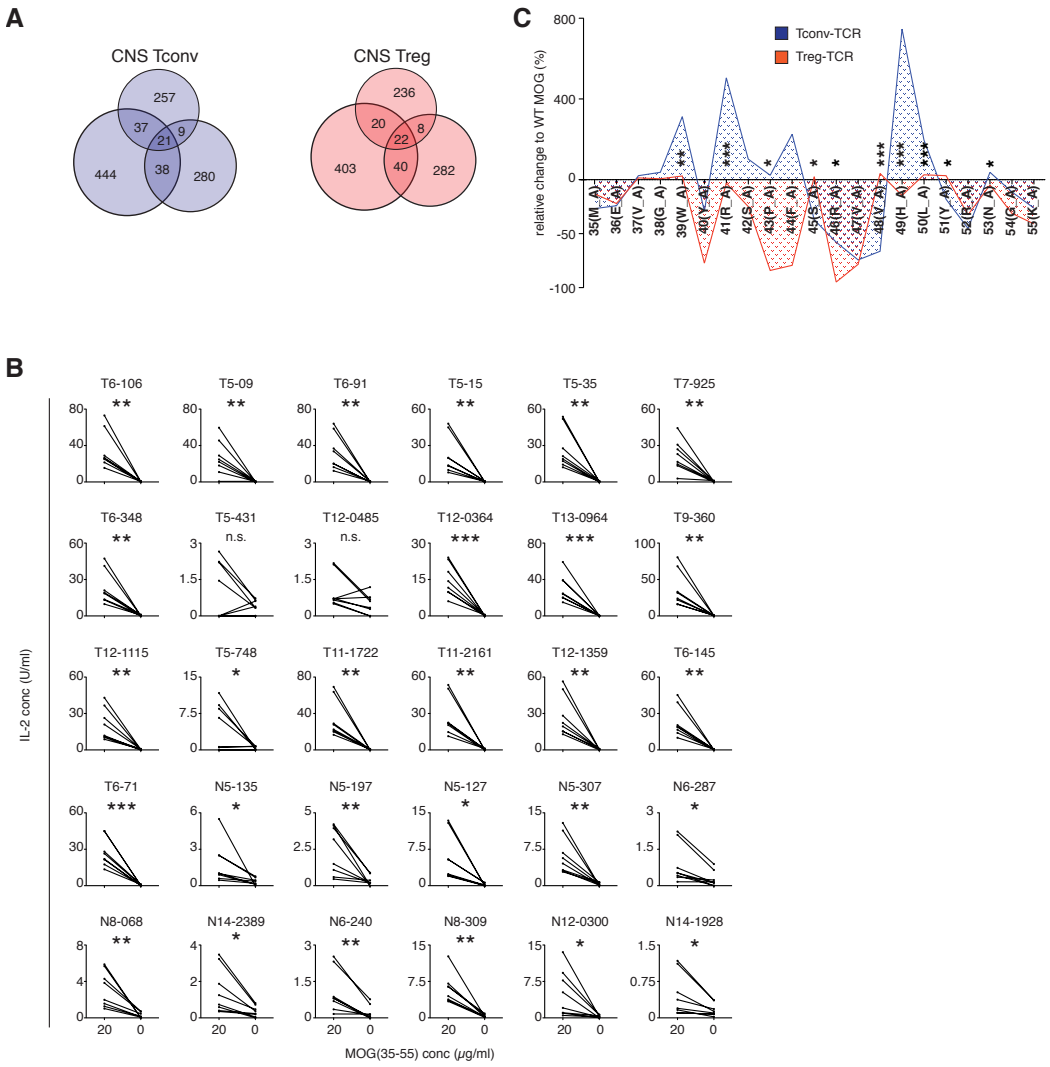

Figure S2, related to Figure 2 | Antigen recognition by TCR from MOG-reactive Tregs and Tconvs.

A. Venn diagram showing the numbers of unique TCRα sequences cloned from Tconvs and Tregs from the CNS of Kaa.Foxp3.eGFP.TCRβ$^{+/-}$TCRα$^{+/-}$ mice with EAE in each of the three independent experiments. The overlaps indicate sequences found in more than one experiment. **B.** T.54ζ17 cell lines expressing 30 distinct TCR (19 from Tregs, 11 from Tconvs) were stimulated with splenic APCs loaded with 20 μg/ml MOG(35-55) (left) or no peptide (right) for 48 h, and IL-2 concentrations in supernatants were determined by ELISA. Data are pooled from four experiments each performed with two independent T cell lines for each TCR. **C.** A set of randomly

selected T cell lines expressing Treg (n=7) or Tconv (n=6) TCR were stimulated for 48 h with the 21 variants of alanine-substituted MOG peptide, and the WT MOG(35-55) peptide at 2 μg/ml. Data show the change of IL-2 secretion upon stimulation with each altered peptide compared to the original peptide for Tregs and Tconvs TCR. Asterisks indicate substitutions leading to significantly altered responses for the Treg vs. Tconv TCR (unpaired t-test). One representative out of two experiments.

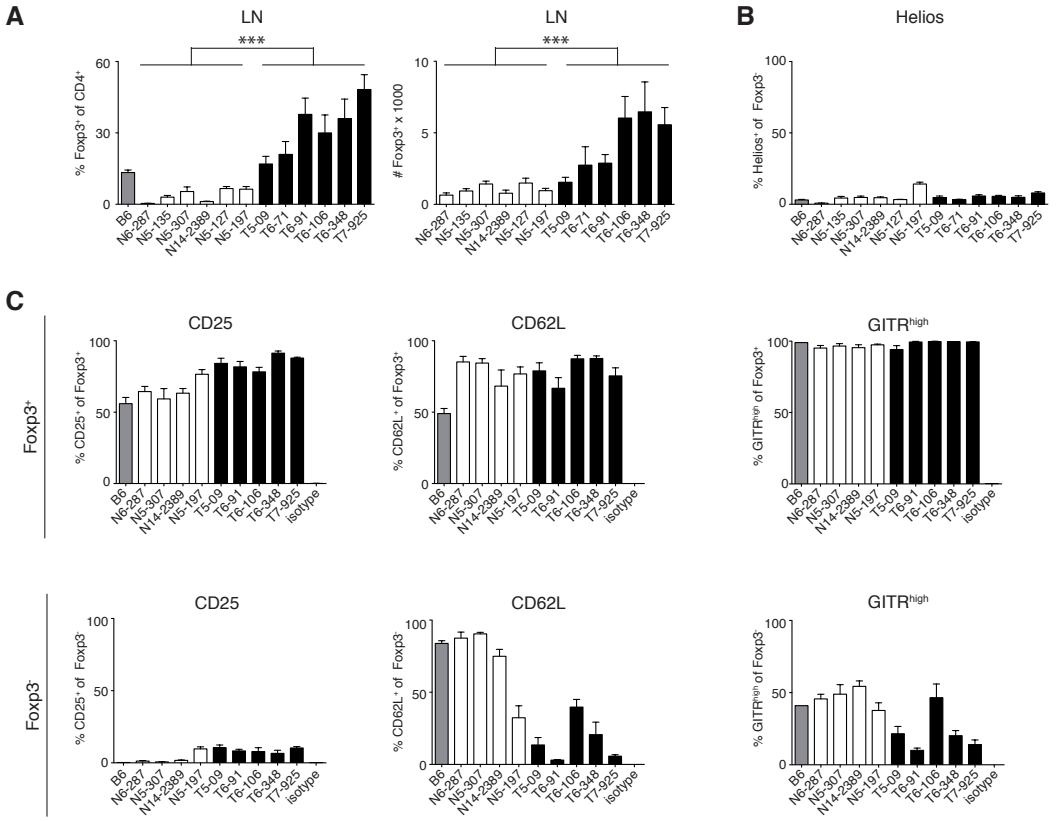

Figure S3, related to Figure 3 | Instructive role of the TCR for MOG-reactive Treg development.

This supplementary figure provides complementary information on the retrogenic mice described in Figure 3. **A.** Nine weeks after reconstitution LN were analysed for percentage among donor-derived CD45.2$^+$CD4$^+$ T cells (left) and absolute number (right) of donor-derived CD45.2$^+$CD4$^+$Foxp3$^+$ cells. Data were analysed comparing all mice prepared with Tconv TCR vs. all mice made with Treg TCR (unpaired t-test). **B.** Expression of Helios by splenic donor-derived CD45.2$^+$Foxp3$^-$ Tconvs was determined by flow cytometry. **C.** Donor-derived splenic CD45.2$^+$CD4$^+$Foxp3$^+$ Tregs (top) and CD45.2$^+$CD4$^+$Foxp3$^-$ Tconvs (bottom) were analysed by flow cytometry for expression of CD25, CD62L and GITR. Black bars: Treg TCR. White bars: Tconv TCR. Data show mean + sem and are pooled from two experiments (n=9/10 per TCR).

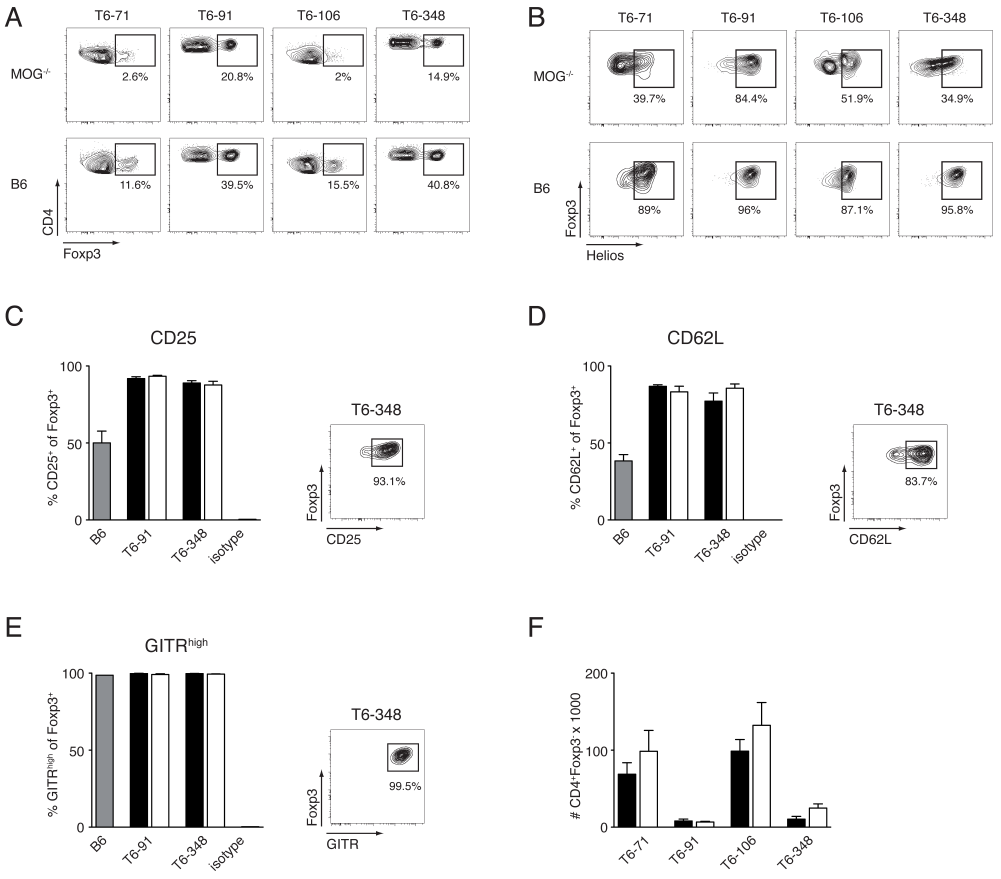

Figure S4, related to Figure 4 | Endogenous MOG controls the selection of MOG-reactive Tregs.

This supplementary figure provides complementary information on the retrogenic mice described in Figure 4. **A.** Representative FACS plots showing expression of Foxp3 by donor-derived $CD45.1^+CD4^+$ T cells in spleen in reconstituted $MOG^{-/-}$ (upper row) or C57BL/6 mice (lower row). Numbers indicate the percentage of $Foxp3^+$ cells in gated $CD45.1^+CD4^+$ T cells. **B.** Representative FACS plots showing expression of Helios and Foxp3 in $CD45.1^+CD4^+Foxp3^+$ Tregs in spleen of reconstituted $MOG^{-/-}$ (upper row) or C57BL/6 mice (lower row). Numbers indicate the percentage of $Helios^+$ cells. **C.-E.** Expression of CD25, CD62L and GITR on splenic $CD45.1^+CD4^+Foxp3^+$ Tregs (left) and representative FACS plots from retrogenic C57BL/6 mice reconstituted with cells expressing the TCR T6-348 (right). **F.** Absolute

number of donor-derived $CD45.1^{+}CD4^{+}Foxp3^{-}$ Tconvs in the spleen of retrogenic mice.

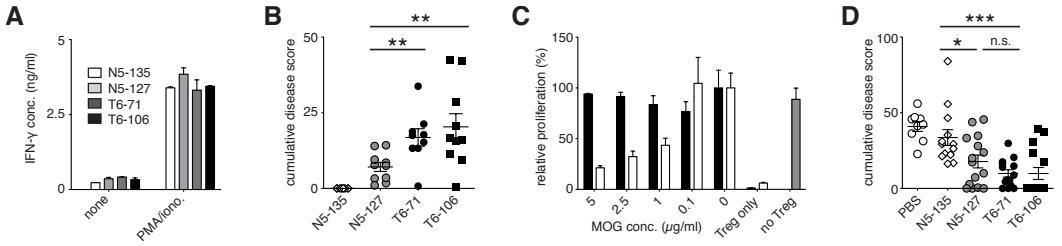

Figure S5, related to Figure 5 | TCR functional avidity determines the function of MOG-reactive Tregs and Tconvs.

A. $CD4^+CD25^-$ Tconvs were transduced with retroviral vectors encoding for one of four different MOG-reactive TCR (N5-135, N5-127, T6-71, T6-106), and subsequently stimulated or not with PMA/ionomycin for 24 h. IFN-γ concentration in supernatant was measured by ELISA. Values show means of duplicates + sem. One representative of two experiments. **B.** Data show the cumulative disease scores for the groups of mice shown in Figure 5D, and are pooled from two experiments. **C.** $CD4^+$ T cells from OT-II TCR-transgenic mice were activated with OVA(323-339) peptide (2 µg/ml) for three days in the presence of polyclonal Tregs transduced to express the T6-106 TCR and different amounts of MOG(35-55). Proliferation was measured by ^{3}H-thymidine incorporation, and standardized relatively to cultures not containing Tregs (100%). Bars show means of duplicates + sem. One representative of two experiments. **D.** Data show the cumulative disease scores for the groups of mice shown in Figure 5F, and are pooled from three experiments.

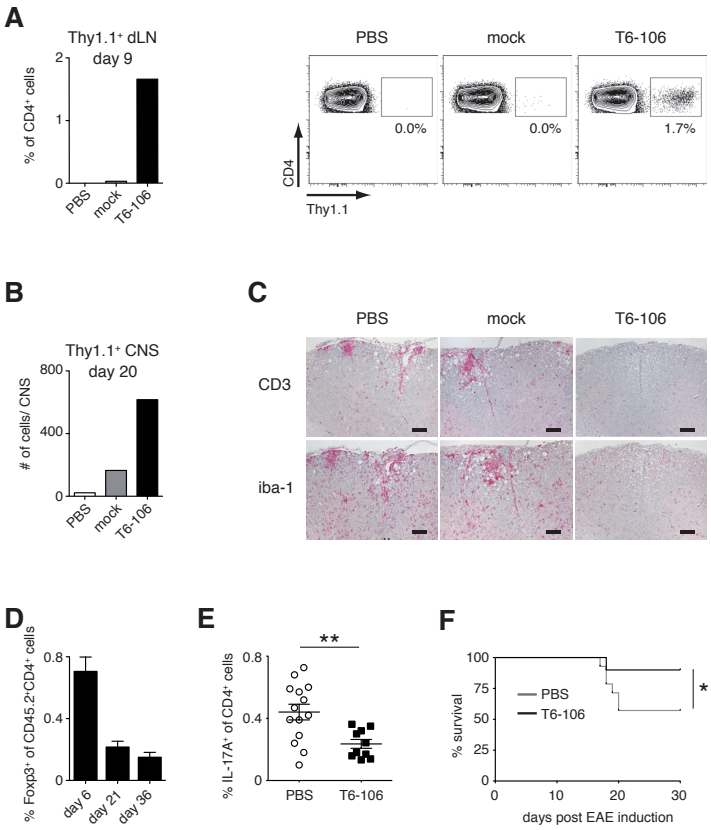

Figure S6, related to Figure 6 | Protective effect of engineered MOG-reactive Tregs in EAE.

This supplementary figure provides complementary information for the experiments described in Figure 6. **A.** Data show percentages of transduced Thy1.1$^+$ cells among total CD4$^+$ T cells in draining LN (popliteal and inguinal), and representative stainings for expression of CD4 and Thy1.1 among CD4$^+$ T cells, for the mice analysed in Figure 6A. **B.** Data show absolute numbers of transduced Thy1.1$^+$ T cells in CNS (brain and spinal cord) of mice shown in Figure 6B analysed on day 20 after EAE induction. One representative of two experiments. **C.** Immunohistochemistry of spinal cord sections from Treg-treated and control mice collected on day 20 after EAE induction, as in (B). **D.** Naïve CD45.1$^+$ C57BL/6 mice received 2x10^6 T6-106 TCR-modified CD45.2$^+$ Tregs (n=4) or PBS (n=5), and persistence of the cells in blood was followed over time. Shown is the percentage of CD45.2$^+$Foxp3$^+$ cells among total CD4$^+$ cells. One representative of two experiments. **E.** Mice from the experiment

shown in Figure 6D were bled on day 10 after immunization, and blood samples were re-stimulated with MOG(35-55) for 5 h to quantify the percentage of IL-17A-secreting cells among $CD4^+$ cells by flow cytometry. Data pooled from two experiments. **F.** Survival curves of mice from Figure 6D. Data pooled from two experiments.

Sequence ID	V	CDR3	J
T5-15*	TRAV4D-3*03	CAAELTGNTGKLIF	TRAJ37*01
T5-35*	TRAV4D-3*03	CAASNTNKVVF	TRAJ34*02
T5-431	TRAV4D-3*03	CAAEHRNYQLIW	TRAJ33*01
T5-748	TRAV4D-3*03	CAAEPARSNAKLTF	TRAJ42*01
T5-9	TRAV4D-3*03	CAAEVAGNTGKLIF	TRAJ37*01
T6-106*	TRAV7D-2*02	CAASGANTGKLTF	TRAJ27*01
T6-145	TRAV4D-3*03	CAAGNSAGNKLTF	TRAJ17*01
T6-348	TRAV4D-3*03	CAAGNSNNRIFF	TRAJ31*01
T6-71	TRAV7D-2*02	CAASGANTGKLTF	TRAJ52*01
T6-91	TRAV4D-3*03	CAAEITGNTGKLIF	TRAJ37*01
T7-925	TRAV4D-3*03	CAADGGSNAKLTF	TRAJ42*01
T9-360	TRAV4D-3*03	CAANYAQGLTF	TRAJ26*01
T11-1722	TRAV4D-3*03	CAADYANKMIF	TRAJ47*01
T11-2161	TRAV7D-2*02	CAASKANTGKLTF	TRAJ27*01
T12-0364	TRAV4D-3*03	CAAPGNTGKLIF	TRAJ37*01
T12-0485	TRAV6N-7*01	CALGSYQGGRALIF	TRAJ15*01
T12-1115	TRAV4D-3*03	CAAEYNQGKLIF	TRAJ23*01
T12-1359	TRAV4D-3*03	CAAEAGNNRIFF	TRAJ31*01
T13-0964	TRAV4D-3*03	CAASNYQLIW	TRAJ33*01
N5-127	TRAV4D-3*03	CAARNTNTGKLTF	TRAJ27*01
N5-135	TRAV13N-1*01	CAMGGGSNAKLTF	TRAJ42*01
N5-197	TRAV4D-3*03	CAATASSSFSKLVF	TRAJ50*01
N5-307	TRAV4N-3*01	CAAGNYNVLYF	TRAJ21*01
N6-240	TRAV4N-4*01	CAAGNSAGNKLTF	TRAJ17*01
N6-287	TRAV13-2*02	CAPTNSAGNKLTF	TRAJ17*01
N8-068	TRAV4N-3*01	CAARNTNTGKLTF	TRAJ27*01
N8-309	TRAV4D-3*03	CAAGNYNVLYF	TRAJ21*01
N12-0300	TRAV13D-1*02	CAFFNSAGNKLTF	TRAJ17*01
N14-1928	TRAV7D-2*02	CAASPGNTGKLIF	TRAJ37*01
N14-2389	TRAV7D-2*02	CAGGTGNTGKLIF	TRAJ37*01

Table S1, related to Figure S2B | List of TCRα chains tested for MOG reactivity.

This table provides the Vα-CDR3-Jα usage for the TCRα chains from Tregs and Tconvs that were re-expressed in T.54ζ17 cells (Figure S2B). Asterisks mark those sequences found in all three experiments in both subsets.

Supplemental experimental procedures

Mice

C57BL/6J mice were purchased from Charles River and Janvier. $Rag^{-/-}$ (B6.129S7-$Rag1^{tm1Mom}$), $Rag^{-/-}$CD45.1 (B6.SJL(129S6)-*Ptprc*^{a}/BoyCrTac-*Rag2*^{tm1Fwa}), B6.CD45.1 (B6.SJL-*Ptprc*^{a}/BoyAiTac) were bred under specific pathogen-free conditions at the Bundesinstitut für Risikobewertung (Berlin, Germany). $MOG^{-/-}$ (MOGi-cre) (Hovelmeyer et al., 2005) mice were a kind gift of A. Waisman (Universitätsmedizin Mainz, Germany). Kaa mice express the public TCRβ chain (TRBV13-2/TRBD2, TRBJ2-1, CDR3: CASGETGNNYAEQFF (Fazilleau et al., 2006). This TCRβ was amplified from the P32.2 MOG-reactive hybridoma (Sweenie et al., 2007), and cloned into the huCD2 minigene vector (Zhumabekov et al., 1995), which was used to generate the transgenic Kaa mouse. In brief, DNA was injected at a concentration of 2 ng/μl into the pronucleus of donor zygotes from superovulated 5-6 weeks old C57BL/6J female mice. Subsequently, 2-cell stage embryos were transferred into the oviducts of pseudopregnant CD1 recipients. Kaa mice were crossed to Foxp3.IRES.eGFP (Wang et al., 2008) and $TCR\alpha^{-/-}TCR\beta^{-/-}$ mice (Mombaerts et al., 1992) to obtain Kaa .Foxp3.IRES.eGFP^{+}$TCR\alpha^{+/-}TCR\beta^{+/-}$ mice.

Peptides used for active EAE induction and *in vitro* assays

MOG(35-55) peptide (MEVGWYRSPFSRVVHLYRNGK), OVA(323-339) (ISQAVHAAHAEINEAGR) peptide, and the alanine-substituted 49(H_A) peptide variant used for immunization experiments were produced at the Institut für Medizinische Immunologie, Charité (Berlin, Germany). The alanine-

modified peptides used for *in vitro* stimulation assays were obtained from JPT Peptide Technologies (Germany).

Antibodies and Flow cytometry

After blocking of Fc receptors (2.4G2), surface stainings were done with mAbs against CD3 (145-2C11), CD4 (GK1.5/RM4-5), CD8α (53-6.7), CD19 (6D5), CD45.1 (A20), CD45.2 (104), Thy1.1 (OX-7) Vβ8.1/8.2 (KJ16-133.18), Vβ8.2/8.3 (CT8E), CD49d (R1-2), CD25 (PC61), GITR (DTA-1) and CD62L (MEL-14). For intracellular stainings, cells were fixed and permeabilized with Cytofix/Cytoperm kit (BD Bioscience, San Jose, CA, USA) or Foxp3 staining buffer set (eBioscience, San Diego, CA, USA) and stained with mAbs against IFN-γ (XMG1.2), TNF-α (MP6-XT22), IL-17A (TC11-18H10.1), GM-CSF (MP1-22E9), CD40L (MR1), CTLA-4 (UC10-4B9), Foxp3 (FJK-16s), and Helios (22F6). Antibodies were from Biolegend (San Diego, CA, USA), eBioscience, BD, Miltenyi Biotec (Bergisch Gladbach, Germany) or produced in our facility. MOG-I-A(b) (loaded peptide MOG(38-49): GWYRSPFSRVVH) conjugated to PE and control-I-A(b) tetramers (loaded peptide CLIP(87-101): PVSKMRMATPLLMQA) conjugated to APC were obtained from NIH tetramer facility. For staining, 10^6 cells were incubated for 3 h at 37 °C with 5 µl tetramer in 0.5 ml RPMI medium. Data were acquired on FACS Calibur, LSRII or CantoII (BD) and analyzed with FlowJo software (Tree Star Inc., Ashland, OR, USA). Flow cytometry was performed according to standard procedure (Shen et al., 2014).

Retroviral transduction

Viral particles for transduction of HSC and primary Tregs and Tconvs were produced using Plat-E cells (Morita et al., 2000), which constitutively encode for packaging and envelope proteins, through transient transfection with the MP71 retrovirus vector using $CaPO_4$ precipitation. Supernatants containing retroviral particles were harvested at 48 h and 72 h after transfection, and subsequently used for transduction of HSC, Tconvs, or Tregs.

$CD4^+CD25^+$ Tregs and $CD4^+CD25^-$ Tconvs cells were isolated from spleen and LN of naïve C57BL/6 mice and stimulated in non-tissue culture plates coated with 1 µg/ml anti-CD3 and anti-CD28 (Biolegend). Cells were cultured with 750 or 40 U/ml recombinant human IL-2 (Chiron, Germany), respectively, and transduced on day 2 and 3 after isolation by spinoculation in plates coated with RetroNektin (TaKaRa Biomedicals, Japan). Four to six days after isolation cells were used for adoptive transfer.

Retroviral supernatant for T.54ζ17 cells was produced with HEK-293T cells by transient $CaPO_4$ transfection with pCgp (Soneoka et al., 1995), MLV-eco, and pMY-TCRα-IRES-eGFP or pMig-Kaa-TCRβ-Tomato, respectively. Cells were sequentially transduced to express TCRβ and TCRα and $Tomato^+eGFP^+$ and subsequently sorted.

Passive EAE induction

For induction of passive EAE with *in vitro*-primed Teff cells, splenic and LN lymphocytes of naïve Kaa or C57BL/6 mice were depleted of $CD25^+$ cells by

separation on autoMACS (Miltenyi Biotech) and stimulated *in vitro* for 3 days with 10 µg/ml MOG(35-55) peptide, recombinant mouse IL-2 (10 U/ml), IL-12 and IL-18 (each at 25 ng/ml). $10x10^6$ *in vitro*-primed cells were then injected into naïve C57BL/6 mice intravenously to induce EAE. These mice additionally received 240 ng Pertussis toxin intravenously on days 0 and 2 after cell transfer.

For induction of passive EAE with *in vivo*-primed Kaa cells, Kaa mice were immunized with MOG(35-55), as previously described (Fillatreau et al., 2002). Draining LN were harvested 8 days after immunization, and cells were re-stimulated *in vitro* for 3 days with 10 µg/ml MOG(35-55) peptide, recombinant mouse IL-2 (10 U/ml), IL-12 and IL-18 (each at 25 ng/ml). $6x10^6$ cells were then injected into naïve C57BL/6 mice intravenously to induce EAE. These mice additionally received 240 ng Pertussis toxin intravenously on days 0 and 2 after cell transfer.

For production of transduced MOG-reactive Tconvs by TCR gene transfer, LN and spleen were collected from naïve C57BL/6 mice, subjected to a mouse $CD4^+$ T cell pre-enrichment EasySep kit (STEMCELL technologies), and $CD25^+$ cells were subsequently eliminated using a mouse CD25 positive selection EasySep kit (STEMCELL technologies). The obtained cells were then activated with anti-CD3 (1 µg/ml), anti-CD28 (0.1 µg/ml), IL-2 (40U/ml), IL-12 (25 ng/ml), and IL-18 (25 ng/ml), and transduced at 48 h and 72 h with MP71 retroviral particles, and used *in vitro* or in adoptive transfer at 96 h (1-

$2x10^6$ cells/mouse). Recipient mice additionally received 240 ng Pertussis toxin intravenously on days 0 and 2 after cell transfer.

Treg adoptive transfers

For experiments described in Figure 1F, Tregs were isolated from pooled spleen and LN from naïve C57BL/6 or Kaa mice using a Dynabeads® Untouched™ Mouse CD4 Isolation kit (Life technologies). The untouched fraction was then used to isolate $CD25^+$ cells using biotinylated anti-CD25 (BD Pharmingen) and biotin-magnetic beads (Miltenyi Biotech). Mice were immunized 12-14 h after the Treg transfer.

For experiments described in Figure 1G and Figures 5-7, LN and spleen were collected from naïve C57BL/6 mice, subjected to a mouse $CD4^+$ T cell pre-enrichment EasySep kit (STEMCELL technologies), and $CD25^+$ cells were subsequently obtained using a mouse CD25 positive selection EasySep kit (STEMCELL technologies). For Figure 1G, the isolated Tregs were labelled with 10 µM Cell proliferation dye eFluor450 (eBioscience). C57BL/6 mice received $2\text{-}3x10^5$ Tregs intravenously, and were immunized immediately. For Figures 5-7, the isolated cells were activated on anti-CD3/anti-CD28-coated plates in presence of IL-2 (750 U/ml), and transduced on day 2 and 3 with MP71 retroviral supernatants. C57BL/6 mice received $2x10^5$ $Foxp3^+Thy1.1^+$ transduced Tregs for prophylactic treatments (Figure 5F, 5G, 6A-6B, and 7), and $2x10^6$ $Foxp3^+Thy1.1^+$ transduced Tregs for therapeutic treatment (Figure 6C) and for the experiment described in Figure 6D.

Proliferation assay of CD25-depleted Kaa splenocytes

Complete or CD25–depleted naïve Kaa splenocytes were stimulated in 96 well-plates ($8x10^5$ cells/well) with MOG(35-55) in indicated amounts, and 48 h later 1 mCi ^{3}H-thymidine was added per well. Proliferation was quantified after an additional 18 h with a Top-count NXT liquid scintillation counter (Perkin Elmer). $CD25^+$ cells were depleted via magnetic cell sorting using biotinylated anti-CD25 and anti-biotin magnetic beads (Miltenyi Biotec).

Preparation of mononuclear cells from CNS

Brain and spinal cord were removed from perfused mice and digested with collagenase (Worthington Biochemical) and DNase (Sigma) followed by mechanical disaggregation. Mononuclear cells were isolated on a 30% Percoll gradient (GE Healthcare) by centrifugation for 20 min at 2000 rpm.

Immunohistochemistry

Sections of 1-2 µm of formalin-fixed, paraffin-embedded spinal cord tissue were deparaffinized, and subjected to heat-induced epitope retrieval. T cells and activated microglia were stained with polyclonal rabbit antibodies against either CD3 (Dako) or iba-1 followed by detection with biotinylated donkey anti-rabbit antibody (Dianova) and the $LSAB^+$, Dako REAL™ Detection System using Fast Red as chromogen (Dako). Scale bar size is 100 µm.

Detection of cytokine production by ELISA and intracellular cytokine staining

TCR-expressing T.54ζ17 cells were seeded in 96-well flat-bottom plates (10^4 cells/ well) together with either MOG(35-55) or one of the alanine-substituted MOG peptides (2 µg/ml), except if otherwise indicated, and $3x10^5$ irradiated splenic APCs. Supernatants were harvested after 48 h, and IL-2 concentration in supernatant was measured by ELISA, as previously described (Calderon-Gomez et al., 2011).

For detection of CD40L, IFN-γ, IL-17A, and GM-CSF expression by blood $CD4^+$ T cells, blood was collected and immediately subjected to red blood cell lysis. Cells were subsequently stimulated in 96-well flat bottom plates at $6x10^5$ cells / well with 20 µg/ml MOG(35-55) for 6 h in the presence of GolgiStop (BD Biosciences). Cells were then stained as previously described (Calderon-Gomez et al., 2011).

For detection of IFN-γ, IL-17A, TNF-α, and GM-CSF expression by Kaa $CD4^+$ T cells (Figures 1A and B), activated cells were re-stimulated on day 3 of culture with PMA/Ionomycin (Sigma) for 5 h in the presence of Golgi stop (BD Pharmingen). Cells were then stained as previously described (Calderon-Gomez et al., 2011).

IFN-γ was quantified in cell supernatant after 24 h of cultures using a BD OptEIA ELISA kit.

Sequences of miRNA for knock-down of CD49d, GITR and control miRNA

The *Cd49d*-specific antisense sequence was TGA ACA GTC AGC ATA ACC TCA, which was inserted into two different miRNA environments. The *Tnfrsf18*-specific antisense sequences AAT CCA AAC TGA GAA CAG TTG and AAC AGT TGG TCC AAA GTC TGC were inserted into the miR-155 and the artificial miRNA, respectively. Control miRNAs were generated by inserting the antisense sequence AAA TTA TTA GCG CTA TCG CGC into the same two environments.

Supplemental references

Calderon-Gomez, E., Lampropoulou, V., Shen, P., Neves, P., Roch, T., Stervbo, U., Rutz, S., Kuhl, A.A., Heppner, F.L., Loddenkemper, C.*, et al.* (2011). Reprogrammed quiescent B cells provide an effective cellular therapy against chronic experimental autoimmune encephalomyelitis. European journal of immunology *41*, 1696-1708.

Fazilleau, N., Delarasse, C., Sweenie, C.H., Anderton, S.M., Fillatreau, S., Lemonnier, F.A., Pham-Dinh, D., and Kanellopoulos, J.M. (2006). Persistence of autoreactive myelin oligodendrocyte glycoprotein (MOG)-specific T cell repertoires in MOG-expressing mice. European journal of immunology *36*, 533-543.

Fillatreau, S., Sweenie, C.H., McGeachy, M.J., Gray, D., and Anderton, S.M. (2002). B cells regulate autoimmunity by provision of IL-10. Nature immunology *3*, 944-950.

Hovelmeyer, N., Hao, Z., Kranidioti, K., Kassiotis, G., Buch, T., Frommer, F., von Hoch, L., Kramer, D., Minichiello, L., Kollias, G.*, et al.* (2005). Apoptosis of oligodendrocytes via Fas and TNF-R1 is a key event in the induction of experimental autoimmune encephalomyelitis. Journal of immunology *175*, 5875-5884.

Mombaerts, P., Clarke, A.R., Rudnicki, M.A., Iacomini, J., Itohara, S., Lafaille, J.J., Wang, L., Ichikawa, Y., Jaenisch, R., Hooper, M.L., and et al. (1992). Mutations in T-cell antigen receptor genes alpha and beta block thymocyte development at different stages. Nature *360*, 225-231.

Morita, S., Kojima, T., and Kitamura, T. (2000). Plat-E: an efficient and stable system for transient packaging of retroviruses. Gene therapy *7*, 1063-1066.

Shen, P., Roch, T., Lampropoulou, V., O'Connor, R.A., Stervbo, U., Hilgenberg, E., Ries, S., Dang, V.D., Jaimes, Y., Daridon, C.*, et al.* (2014). IL-35-producing B cells are critical regulators of immunity during autoimmune and infectious diseases. Nature *507*, 366-370.

Soneoka, Y., Cannon, P.M., Ramsdale, E.E., Griffiths, J.C., Romano, G., Kingsman, S.M., and Kingsman, A.J. (1995). A transient three-plasmid expression system for the production of high titer retroviral vectors. Nucleic acids research *23*, 628-633.

Sweenie, C.H., Mackenzie, K.J., Rone-Orugboh, A., Liu, M., and Anderton, S.M. (2007). Distinct T cell recognition of naturally processed and cryptic epitopes within the immunodominant 35-55 region of myelin oligodendrocyte glycoprotein. Journal of neuroimmunology *183*, 7-16.

Wang, Y., Kissenpfennig, A., Mingueneau, M., Richelme, S., Perrin, P., Chevrier, S., Genton, C., Lucas, B., DiSanto, J.P., Acha-Orbea, H.*, et al.*

(2008). Th2 lymphoproliferative disorder of LatY136F mutant mice unfolds independently of TCR-MHC engagement and is insensitive to the action of Foxp3+ regulatory T cells. Journal of immunology *180*, 1565-1575.

Zhumabekov, T., Corbella, P., Tolaini, M., and Kioussis, D. (1995). Improved version of a human CD2 minigene based vector for T cell-specific expression in transgenic mice. Journal of immunological methods *185*, 133-140.